



WINPEC Working Paper Series No. E2507

May 2025

Climate Change and the Decline of Labor Share

Xincheng Qiu Masahiro Yoshida

Waseda INstitute of Political EConomy
Waseda University
Tokyo, Japan

Climate Change and the Decline of Labor Share^{*}

Xincheng Qiu[†]

Masahiro Yoshida[‡]

November 19, 2024

([click here for latest version](#))

Abstract

We study the impact of climate change on the labor share. Using a newly constructed dataset combining US county-level labor shares with climate variables, we find that extreme temperatures reduce labor share. This adverse effect is more pronounced in industries with higher outdoor exposure and automation potential. We also show that extreme temperatures accelerate the adoption of industrial robots. Overall, climate change accounts for 14% of the decline in labor share during 2001–2019. In the last century, however, the opposing effects of decreased cold days and increased hot days offset each other, consistent with the well-documented constancy of labor share.

Keywords: climate change, labor share, automation

JEL Codes: E25, Q54, O33

^{*}We thank seminar participants at Waseda for useful comments.

[†]Guanghua School of Management, Peking University. Email: xincheng.qiu@gsm.pku.edu.cn. Webpage: www.xinchengqiu.com.

[‡]Department of Political Science and Economics, Waseda University, Tokyo. Email: m.yoshida@waseda.jp. Webpage: www.m-yoshida.com.

1 Introduction

The labor share—the portion of national income accruing to workers as wages and compensation—has fallen sharply in the United States since 2000 (as shown by the black line in Figure 1a). This decline disrupts the historical stability of the labor share established as one of Kaldor (1961)’s stylized facts of economic growth, and has been documented across a wide range of countries worldwide (Karabarbounis and Neiman, 2014). Concerns over growing inequality between laborers and capitalists have sparked considerable debate among economists about the causes of this phenomenon, such as technological change, globalization, shifts in market structure, and various measurement issues (see Grossman and Oberfield, 2022, for a review). This paper introduces a novel perspective by uncovering the role of climate change—another prominent global secular trend—in shaping the observed decline of the labor share.

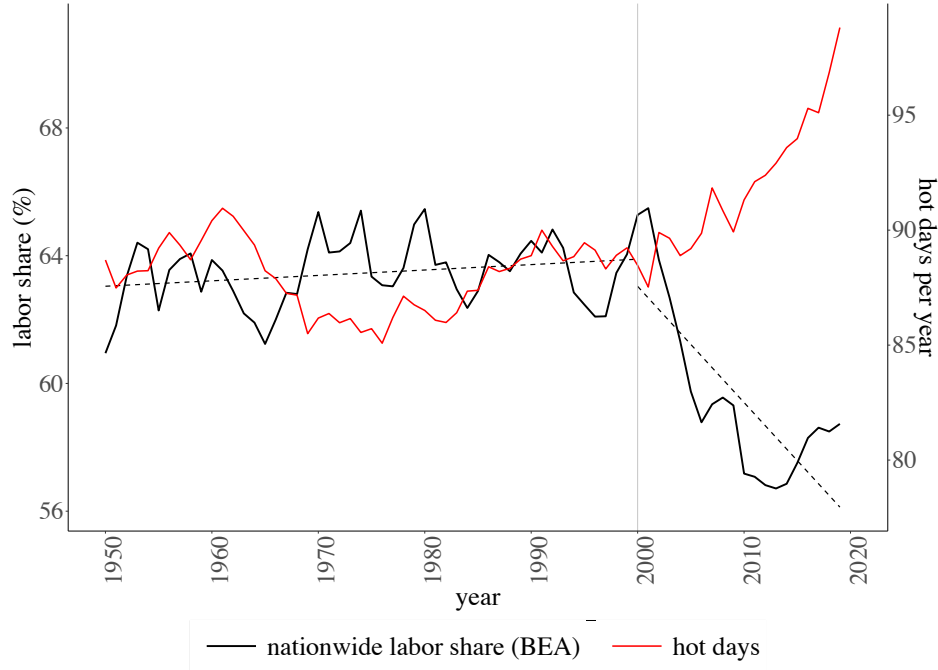
The Earth’s climate is changing rapidly, and the US is no exception to the trend of intensifying global warming in recent decades (as shown by the red line in Figure 1a). Economists are increasingly concerned with the economic consequences of climate change, as global warming and more frequent extreme heat events not only harm ecosystems but also impair production processes. Extreme temperatures cause discomfort for workers, leading to irritability, difficulty concentrating, and physical fatigue. These adverse effects reduce work efficiency, diminish workplace morale, and increase error rates, along with heat strokes and other workplace injuries. We hypothesize that firms are incentivized to adopt labor-saving technologies in response to climate change, which in turn contributes to the decline in labor share.

To empirically test this hypothesis, we build a new county-level panel dataset that combines climate variables constructed from granular daily weather station records, with local labor share constructed from the Bureau of Economic Analysis (BEA) Regional Economic Accounts. To the best of our knowledge, this is the first paper to measure labor share at the county or commuting zone level in the US. Figure 1b presents a scatterplot of local labor share against the ten-year average of hot days per year across commuting zones. The fitted line reveals a clear negative correlation, indicating that hotter cities—such as Atlanta, Dallas, and Houston—tend to have lower labor shares.

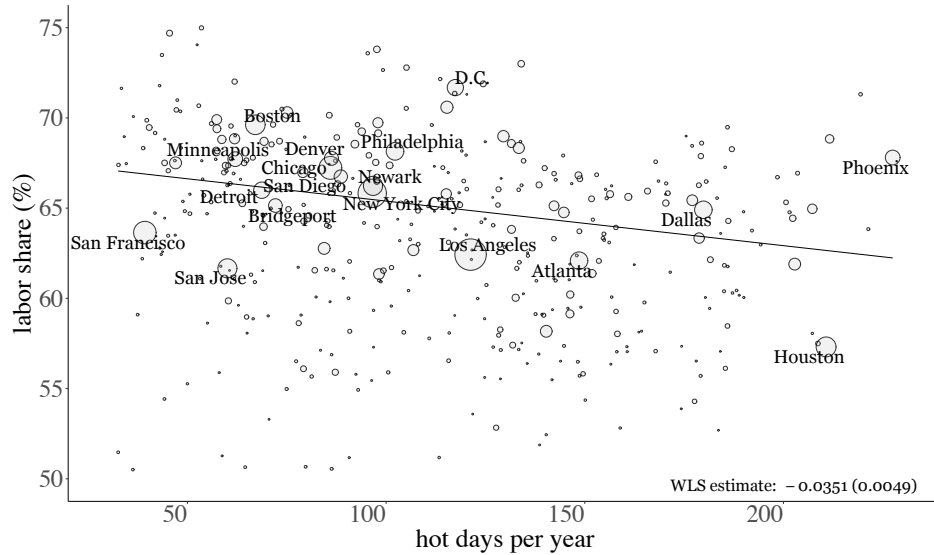
Motivated by Figure 1, we aim to estimate the impact of climate change on the decline in labor share. Even though regional climate change is arguably exogenous, we control for an extensive set of covariates to ensure this. Leveraging granular spatial variation in climate exposure and labor share dynamics, we further include flexible fixed effects at the county, state-by-year, and industry-by-year levels. In the preferred specification, we find that an additional 10 hot days above 77°F and 10 cold days below 50°F per year reduce labor share by 0.59 and 0.87 percentage points, respectively. These results are robust across a wide range of alternative specifications.

Figure 1: Climate Change and Labor Share in the US

(a) Nationwide Time Trend (1950–2019)



(b) Cross-Regional Relationship (2019)



Notes: Panel (a): County-level exposure to hot days is aggregated at the national level, weighted by county employment in 2000 from the County Business Pattern ([Eckert et al., 2021](#)). Hot days are defined as days with an average temperature during working hours (8 a.m. to 6 p.m.) exceeding 77°F. Aggregate labor share is taken from the headline figure provided by the Bureau of Economic Analysis. The dashed lines are trends in 1950–2000 and 2000–2019, respectively. Panel (b): County-level exposure to hot days is aggregated to the commuting zone (CZ) level for the period 2010–2019, weighted by county employment. Each bubble represents a CZ, with its size corresponding to the denominator. Outliers with the share of national GDP below 0.01% or with over 230 or below 30 hot days are excluded. Figure A-6 shows a similar negative relationship at the state level.

We then examine the mechanism through which extreme temperatures suppress labor share—namely, by reducing worker efficiency and incentivizing firms to adopt labor-saving technologies. First, we expect the discomfort caused by extreme temperatures to be more severe in jobs with greater exposure to outdoor tasks or indoor environments without climate control. Second, workers in jobs with higher automation potential—typically those involving manual, routine, and hazardous tasks—are more susceptible to being replaced by machines. Using data on occupational task content, we find support for both predictions. Moreover, employing two datasets from the BEA and the International Federation of Robotics (IFR), we provide direct evidence that industries more exposed to extreme temperatures adopt more industrial robots. Collectively, these results suggest that climate-induced automation contributes to the decline in labor share.

Finally, we evaluate the macroeconomic implications of these findings. We quantify the overall effect of climate change on labor share by multiplying the observed changes in numbers of hot and cold days by their respective estimated coefficients and aggregating the effects. Between 2001 and 2019, the increase in the annual number of hot days (+12.5 days) dominates the decrease in cold days (−1.2 days). Our calculation reveals that these changes lead to an aggregate drop in the labor share of 0.54 percentage points, accounting for 14% of the observed declining trend. In contrast, during the period from 1950 to 2001, the competing effects of the increase in hot days (+9.0 days) and the decrease in cold days (−4.7 days) nearly cancel out each other, consistent with the established stability of labor share in the 20th century.

Related Literature. This paper contributes to three strands of literature. First, it adds to the debate on the decline in labor share. Existing explanations include technological changes (Karabarbounis and Neiman, 2014; Acemoglu and Restrepo, 2018), globalization (Elsby et al., 2013), shifts in market structure (De Loecker et al., 2020; Autor et al., 2020; Kehrig and Vincent, 2021), and measurement issues (Rognlie, 2015; Koh et al., 2020; Gutiérrez and Piton, 2020). This paper highlights a novel fundamental force—climate change—and argues that it has shaped technological change by decreasing labor efficiency. This perspective mirrors Karabarbounis and Neiman (2014), who emphasize that the decline in relative cost of capital has facilitated the substitution of labor with capital. Acemoglu and Restrepo (2018, 2019) argue that automation contributes to the decline in labor share, and our findings suggest that climate change is a driver of the automation process. Importantly, our explanation extends to the stability of labor share in the 20th century.

Second, our proposed mechanism of climate-induced automation represents an unexplored form of directed technological change (Acemoglu, 2002) that is conceptually similar to other examples of rising labor costs driving robot adoption, such as population aging (Acemoglu and

Restrepo, 2022), shortages of low-skilled immigrants (Lewis, 2011), and dismissal regulations (Presidente, 2017). In particular, to the best of our knowledge, we provide the first evidence that exposure to extreme temperature induces the adoption of industrial robots. A conventional narrative in climate science, environmental economics, and policy discussions posits that technological change, particularly since the Industrial Revolution, has caused the climate change. We offer a reverse perspective that climate change has catalyzed technological change.

Third, this paper contributes to the burgeoning literature on the macroeconomic effects of climate change. Previous studies have explored its impact on economic growth (Dell et al., 2012; Nath et al., 2024), factory productivity (Cachon et al., 2012; Chen and Yang, 2019; Somanathan et al., 2021), incomes (Deryugina and Hsiang, 2014), agricultural innovation (Moscona and Sastry, 2022), and structural change via labor reallocation, especially from agriculture to manufacturing (Peri and Sasahara, 2019; Colmer, 2021). To our knowledge, no prior research has connected climate change to the ongoing debate regarding the decline in labor share.

The remainder of the paper is structured as follows. Section 2 describes the data sources used in the study. Section 3.1 presents the baseline results, accompanied by robustness checks in Section 3.2. Section 4.1 discusses the mechanism leveraging occupational characteristics, and Section 4.2 provides industry-level evidence that climate change induces robot adoption. Section 5 assesses the macroeconomic implications of our findings and Section 6 concludes.

2 Data

2.1 Climate Data

We draw on weather station data from the Global Historical Climatology Network Daily (GHCN-Daily), managed by the National Climatic Data Center (NCDC) of the National Oceanic and Atmospheric Administration (NOAA). The GHCN-Daily database provides daily climate statistics, such as maximum and minimum daily temperature, precipitation, and snowfall, from approximately 15,000 weather stations across the US, offering a comprehensive climatic dataset with the highest frequency, resolution, and quality since the 19th century. We use data from stations with complete annual records during 1940–2019.

To aggregate station-level data to the county level, we employ the inverse-distance weighting method (e.g., Barreca et al., 2016). Specifically, for each county we select the three nearest weather stations to the county’s population centroid and aggregate their daily records, weighted by the inverse square of the distance from the centroid. Then, we construct an average daytime temperature for each day d as a weighted average of the maximum and minimum temperature,

i.e., $T_d = \omega T_d^{\max} + (1 - \omega) T_d^{\min}$. Instead of using $\omega = 0.5$ as is common in the climate literature, we assign $\omega = 0.75$ in light of our focus on regular working hours, 8 a.m. to 6 p.m.¹ We obtain a substantial geographical variation of exposure to climate change across counties even within states (see Figure A-2 for descriptive heatmaps).

Each location’s exposure to climate change is measured as the change in the number of hot and cold days per year. There is no consensus on the appropriate temperature cutoffs in defining hot and cold days in the climate literature, and the choice varies depending on the context, such as outcome variables (e.g., mortality, GDP, mobility), samples (e.g., the elderly, babies, or prime-age workers), and countries (e.g., the US, China, or India). Our strategy is to use the upper and lower terciles of the nationwide temperature distribution in the latest decade (Figure A-3). Specifically, hot days are defined as those with an average working-hour temperature above 77°F (25°C) and cold days as below 50°F (10°C).² We show in Table A-2 that the two-tailed estimates are robust to alternative, reasonable cutoff pairs.

2.2 Labor Share

To measure labor share at the county level, we link two data products from the BEA Regional Economic Accounts: GDP by County and Personal Income by County. The county-level GDP data are only available from 2001 onwards. Nevertheless, this period is well-suited for our analysis, as it encompasses the most drastic changes in both climate and labor share, as depicted in Figure 1a. Within each county, the BEA data enable us to construct labor shares for 16 NAICS-based industries. We thus adopt a county-industry cell analysis in our baseline specification. This granular approach is particularly valuable, as counties exhibit significant differences in industrial composition, and industries display substantial heterogeneity in their labor shares.

Specifically, we construct county-level labor shares as the ratio of wage compensation to GDP excluding proprietors’ income, where wage compensation includes both wages and salaries and associated supplements. Accurately allocating self-employment income between labor and capital income poses a well-known measurement challenge. We exclude proprietors’ income from the denominator, thereby focusing on the wage employment sector. Alternatively, this assumes that the self-employed sector has the same labor share as the overall economy, an approach termed the “economy-wide basis” measure by Kravis (1959). We confirm in Figure A-4 that the aggregate of our measure closely tracks both the Bureau of Labor Statistics (BLS)

¹This calculation assumes a linear fluctuation of temperature between its minimum at 6 a.m. and its maximum at 1:30 p.m.

²Graff Zivin and Neidell (2014) use the same cutoff of 25°C for hot days for the US and Chen and Yang (2019) use 24°C for China.

and BEA labor share measures since 2001. Figure A-5 plots a heatmap depicting labor share across counties.

2.3 Covariates

In addition to climate and labor share data, we incorporate a comprehensive set of demographic and socioeconomic controls that may independently affect labor share. These covariates are organized into three groups. First, employment demographics at the commuting zone (Tolbert and Sizer, 1996) by NAICS industry level are constructed from the Population Census and the American Community Survey (ACS), including employment shares by four educational attainment levels, five age bins, four racial and ethnic groups, as well as immigration status, gender, and veteran status. Second, proxies for industry structure at the NAICS industry-by-county level are sourced from the County Business Pattern (CBP) Database (Eckert et al., 2021), including measures of concentration that could influence market power and labor demand. Finally, CZ-level labor market characteristics, including population density, non-labor income, share of renters, and unemployment rate, are constructed from the Population Census and the ACS. Appendix I.3 provides a detailed list of all covariates.

3 Empirical Analysis

3.1 Baseline Results

Model. The baseline model regresses county-by-industry level labor share on the number of hot and cold days for each county, controlling for other climatic factors and a rich set of socioeconomic variables. Specifically, for counties (indexed by l) and industries (indexed by k) during three near-decade intervals (indexed by $I = [\underline{I}, \bar{I}]$ for 1990–2001, 2001–2010, and 2010–2019), we consider the following regression:

$$\text{LaborShare}_{l,k,\bar{I}} = \beta^h \text{hd}_{l,I} + \beta^c \text{cd}_{l,I} + \mathbf{A}\mathbf{C}_{l,I} + \mathbf{\Gamma}\mathbf{Z}_{l,k,\underline{I}} + \delta_l + \delta_{s,I} + \delta_{k,I} + \varepsilon_{l,k,\bar{I}}, \quad (1)$$

where $\text{LaborShare}_{l,k,\bar{I}}$ is county l , industry k 's labor share at the period end \bar{I} . We focus on nonfarm, nonfinancial private industries, as is common in studies on labor share. Treatment variables $\text{hd}_{l,I}$, $\text{cd}_{l,I}$ are the average numbers of hot and cold days in county l during period I , respectively. The coefficients of interest, β^h, β^c , capture the impact of an additional 10 hot or cold days on labor share. A similar two-tail specification has been widely used in, for example, Barreca et al. (2016) and Somanathan et al. (2021). We also control for additional climate

covariates $\mathbf{C}_{l,I}$, including daily precipitation and the number of days with no precipitation, and those with heavy snowfall averaged during each period I .

In addition to county fixed effects δ_l , the model allows for the inclusion of state-by-period fixed effects $\delta_{s,I}$, capturing any time-varying state-level institutions (e.g., unionization, taxation, minimum wage), as well as nationwide industry-by-period fixed effects $\delta_{k,I}$ (e.g., technological evolution, trade competition). Thus, the estimates are derived from within-county and within-industry variations, net of state-year and industry-year level common effects. Moreover, we incorporate a comprehensive set of controls $\mathbf{Z}_{l,k,I}$ that may affect labor share. We include three lists of start-of-period covariates for 1990, 2000 and 2010, as described in Appendix I.3: demographic composition of employment $\mathbf{D}_{c,k,I}$ by commuting zone c and industry k , industry structure $\mathbf{S}_{l,k,I}$ by county l and industry k , and commuting zone c 's local labor market characteristics $\mathbf{M}_{c,I}$, where each commuting zone c consists of several counties l .

The regression is weighted by denominators of labor share, i.e., GDP minus proprietors' income. Since temperature is spatially correlated across counties, standard errors are clustered at the state level. We drop cells with missing labor shares due to unrecorded labor incomes or GDPs. To further avoid potential measurement errors, we restrict our analysis to cells with labor shares between 0 and 1.

Results. Table 1 summarizes the estimates with a variety of inclusion of controls. In the preferred specification from Equation (1) that includes all control variables (Column 5), we find that an increase of 10 hot days in replacement of normal days reduces the labor share by 0.59 percentage points ($t = -2.92$). Although changes in the number of cold days are less prominent in the new century (see Section 5), the effect of cold days is also significantly negative: an additional 10 cold days reduces the labor share by 0.87 percentage points ($t = -2.11$).

Column (1) presents the estimated coefficients for hot and cold days with the full set of fixed effects but with no additional controls. Columns (2)–(5) progressively add controls for climate variables $\mathbf{C}_{l,I}$, demographic compositions $\mathbf{D}_{c,k,I}$, industry structure $\mathbf{S}_{l,k,I}$, and labor market characteristics $\mathbf{M}_{c,I}$. Both the magnitude and precision of the estimates remain remarkably stable across these specifications. This suggests that under the flexible fixed effects at the county, state-year, and industry-year levels, climate shocks are nearly unconditionally-independent of other regional- and industry-level observables. Given the richness of the fixed effects and controls, we believe the estimates are unlikely to be confounded by other factors and interpret these estimates as indicative of the causal impact of climate change.

Sector heterogeneity. The baseline model identifies the average nationwide treatment effect of hot and cold days. Does the climate impact vary across sectors with different degrees of

Table 1: Climate Change and Labor Share (by County-by-NAICS Industries, 2001–2019)

<i>dependent variable: labor shares</i> (units: percentage points)					
	no controls			Baseline	
	(1)	(2)	(3)	(4)	(5)
10 hot days	−0.675 (0.178)	−0.630 (0.159)	−0.638 (0.159)	−0.588 (0.195)	−0.589 (0.202)
10 cold days	−0.896 (0.388)	−0.891 (0.403)	−0.908 (0.396)	−0.859 (0.413)	−0.874 (0.414)
county FE	Yes	Yes	Yes	Yes	Yes
state × year FE	Yes	Yes	Yes	Yes	Yes
NAICS × year FE	Yes	Yes	Yes	Yes	Yes
climate variables	—	✓	✓	✓	✓
demography	—	—	✓	✓	✓
industry structure	—	—	—	✓	✓
labor market	—	—	—	—	✓
Observations	93,452	92,810	92,787	90,311	90,311
Adjusted R ²	0.808	0.808	0.810	0.815	0.815

Notes: Unit of analysis: outcome years (2001, 2010, 2019) × counties × industries. We restrict the analysis to cells with labor shares between 0 and 1. The thresholds for hot and cold days are set at 77°F and 50°F, respectively, based on average temperature during business hours (8 a.m. to 6 p.m.). Numbers of hot and cold days are averaged during each period. The regressions are weighted by the denominator of labor share, i.e., GDP minus proprietors' income. Standard errors in parentheses are clustered at the state level.

outdoor exposure? To explore this, we partition the economy into four broad sectors based on industries' dependence on outdoor operations: construction and mining, manufacturing, low-skilled services (e.g., transportation, retail, health care, restaurants), and high-skilled services (e.g., business, information). This classification is both intuitive and corroborated by occupational characters from the Work Context Survey (see Section 4). We extend Equation (1) by interacting $hd_{l,I}$ and $cd_{l,I}$ with sectoral dummies to obtain sector-specific estimates. Notably, the effect of hot days is strictly increasing in the intensity of climate exposure, while cold days exhibit similarly negative impacts (see Appendix II.2). Such sectoral heterogeneity also motivates the direct examination of the mechanism via outdoor exposure in Sections 4, and informs our macroeconomic assessments in Section 5.

3.2 Robustness Checks

To further validate our main result presented in Table 1, we conduct a series of robustness checks. In the interest of space, all corresponding tables are relegated to the Online Appendix.

Cutoffs for hot and cold days. In the baseline specification, we define hot and cold days using thresholds of 77°F (25°C) and 50°F (10°C), respectively, based on tertiles of the nationwide temperature distribution. To test the robustness to the cutoffs, we also run specifications with alternative temperature cutoffs of 73, 75, 77, 80°F for hot days, and 35, 40, 45, 50, 55°F for cold days. Across these specifications, we consistently find significant effects of two-tailed temperatures on labor share (Table A-2).

Treatment window. To capture the long-run effects of climate change, we use changes in the decadal averages of hot and cold days in the baseline specification. We also examine alternative treatment windows, ranging from 1 to 5, 15, and 20 years (Table A-3). The adverse effect remains significant for the longer 15- and 20-year windows. However, for the 1-year and 5-year windows, we do not observe significant estimates for extreme temperature days. This aligns with the conventional view that technological changes and capital adjustments occur over the long run.

Measurement of labor share. We measure labor share as the ratio of wage compensation to GDP excluding proprietors' income. Our measurement closely aligns with the headline figures by both the BEA and BLS (Figure A-4). Alternatively, we consider the ratio of wage compensation to GDP, and the ratio of wage compensation plus proprietors' income to GDP. These proxies effectively reflect two extreme assumptions: one in which all proprietors' income is considered capital income, and the other in which it is entirely labor income. The results remain consistent, indicating that the treatment of proprietors' income has a minimal impact on the findings (Table A-4).

Leave-one-out analysis. One potential concern is that the results might be disproportionately driven by the most temperature-sensitive or automatable sectors. To address this concern, we sequentially drop construction/mining/utilities, manufacturing, and transportation from the analysis. We also exclude the Southeast and South regions, the hottest and most humid areas, or the Northwest and West North Central regions, the coldest areas. Reassuringly, the estimates from each of these subsample analyses remain unchanged (Table A-5).

4 Mechanism

4.1 Occupational Characteristics

We propose that the mechanism underlying the climate-labor share nexus operates through reduced worker efficiency and increased labor costs caused by extreme temperatures, which in turn incentivizes firms to adopt labor-saving technologies. To evaluate this mechanism, we put forth two testable predictions. First, occupations differ in their exposure to climatic conditions, depending on the extent of outdoor activities they involve and access to climate control. In occupations with greater exposure to weather, worker discomfort should be more severe, leading to a larger negative impact of extreme temperatures on labor share. Second, occupations also vary in their susceptibility to automation depending on the intensity of manual, routine, and hazardous tasks—activities more readily and desirably performed by machines. Therefore, in occupations with higher automation potential, the adverse effect is expected to be larger. This section tests these two hypotheses.

Temperature Exposure. To measure jobs’ exposure to temperature, we rely on the Work Context Survey (WCS) from the O*NET (Occupational Information Network) database, sponsored by the US Department of Labor. We draw from the section on “physical and social factors that influence the nature of work” to construct four indices that capture different modes of temperature exposure for 873 O*NET-SOC occupations. We use the following questions:

- “How often does this job require *working outdoors*, exposed to all weather conditions?”
- “How often does this job require *working outdoors, under cover* (e.g., structure with roof but no walls)?”
- “How often does this job require *working indoors in non-controlled environmental conditions* (e.g., warehouse without heat)?”
- “How often does this job require *working indoors in environmentally controlled conditions*?”

To each question, respondents answer using a 5-point scale: 5 = Every day; 4 = Once a week or more but not every day; 3 = Once a month or more but not every week; 2 = Once a year or more but not every month; 1 = Never. Combining answers 4 and 5, we compute employment shares for working at least weekly under each mode of temperature exposure. After mapping O*NET-SOC identifiers to occupation codes in the Census and the ACS, we construct a measure of occupational weather exposure, $x_{c,k,L}$, for each commuting zones c , industry k , at the start-

of-period \underline{I} .³

We extend the baseline model (1) by interacting $hd_{l,I}$ and $cd_{l,I}$ with $x_{c,k,\underline{I}}$:

$$\begin{aligned} \text{LaborShare}_{l,k,\bar{I}} = & \beta^h hd_{l,I} + \beta^c cd_{l,I} + \gamma^h hd_{l,I} \times x_{c,k,\underline{I}} + \gamma^c cd_{l,I} \times x_{c,k,\underline{I}} + x_{c,k,\underline{I}} \\ & + \mathbf{\Lambda C}_{l,I} + \mathbf{\Gamma Z}_{l,k,\underline{I}} + \delta_l + \delta_{k,I} + \delta_{s,I} + \varepsilon_{l,k,\bar{I}}. \end{aligned} \quad (2)$$

Recall that the outcome variable, $\text{LaborShare}_{l,k,\bar{I}}$, represents the labor share for county l and industry k at the end of period \bar{I} , and the second line is the same as (1). In Panel A of Table 2, Columns (1)–(4) report the interaction coefficients γ^h , capturing sensitivity to hot days across different modes of temperature exposure. We find significantly negative interaction coefficients for outdoor environments and outdoor environments with cover (e.g., gas stations, mechanic and repair shops). Indoor non-controlled environments, such as manufacturing plants using fire or furnaces, or transportation warehouses where doors are frequently opened, show an even larger negative estimate than outdoor environments; this suggests stronger incentives for automation, possibly through electric-powered indoor industrial robots. In contrast, indoor controlled environments exhibit significantly positive coefficients.⁴ These results indicate that counties or industries with greater temperature exposure, particularly those without air conditioning, experience larger adverse effects from warming.

Automation Potential. The second testable prediction is that regions or industries with higher proportions of occupations prone to automation would experience a larger impact on labor share. To proxy automation potential, we construct four occupation-level indices from independent sources. We then aggregate these indices to the commuting-zone-by-NAICS-industry level for each start-of-period, using occupational employment shares from the 2000 Census and the 2009–2010 stacked ACS as weights. Analogous to Panel A, Panel B of Table 2 reports how the impact of hot days interacts with potential for automation.

In Column (1), following the approach of Peri and Sparber (2009), we use a physical intensity index constructed from questions from the Abilities Survey in O*NET. Specifically, we average an occupation’s “movement and strength” requirements. In Column (2), we build a manual-routine intensity index, based on a widely-used occupational characteristic from Autor and Dorn (2013) and Autor et al. (2003), originally constructed from the Dictionary of Occupational Titles (DOT). We again find significantly negative interaction coefficients. More directly, in Column (3) we use the “technological exposure to robots” index developed by Webb (2019), measuring

³Alternatively, we use intensive-margin proxies based on the imputed weekly frequency of working under each environment across commuting zones and industries, and find similar estimates.

⁴The index for each mode does not sum up to one, as the questionnaire does not measure the exact amount of time allocated to each working condition.

Table 2: Sensitivity of Climate Impacts to Temperature Exposure and Automation Potential

<i>dependent variable: labor share</i> (units: percentage points)				
Panel A: by climate exposure				
	(1)	(2)	(3)	(4)
10 hot days × outdoor	−0.589 (0.323)			
× outdoor with cover		−2.130 (0.564)		
× indoor non-controlled			−0.929 (0.279)	
× indoor controlled				1.250 (0.217)
Observations	90,296	90,296	90,296	90,296
Adjusted R ²	0.818	0.820	0.819	0.818
Panel B: by task characteristics				
	(1)	(2)	(3)	(4)
10 hot days × physical intensity	−0.944 (0.142)			
× manual routine intensity		−0.220 (0.028)		
× technological exposure to robots			−1.160 (0.138)	
× injury and illness risk				−0.959 (0.185)
Observations	90,295	90,296	90,296	90,296
Adjusted R ²	0.817	0.817	0.817	0.819

Notes: Unit of analysis: outcome years (2001, 2010, 2019) × counties × NAICS industries. We restrict the analysis to cells with labor shares between 0 and 1. All models inherit all controls and three-fold fixed effects at the baseline specification (5) from Table 1, supplemented with task characteristics interacted with hot and cold days. See the main text and Appendix I.4 for details on the construction of task characteristics. These indices are constructed at the commuting-zone-by-NAICS-industry level using employment shares from the 2000 Census and the 2009–2010 stacked ACS. In the interest of space, we only report the interaction estimates, γ^h . The regressions are weighted by the denominator of labor share, i.e., GDP minus proprietors' income. Standard errors in parentheses are clustered at the state level.

the overlap between job task descriptions and global patent profiles on robotics by natural language processing. We again observe significantly negative coefficients, suggesting that the negative impact of extreme heat is amplified in tasks that have a higher technical feasibility for robotics. In Column (4), we construct an injury and illness risk proxy based on questions from the WCS.⁵ Our findings confirm that higher physical danger is associated with a larger negative effect of hot days on labor share. This can be attributed to employers or labor unions prioritizing occupational safety, for example by preventing injuries from the misuse of tools (e.g., cutting or burning tools) or illnesses caused by gas, contaminants, or radiation. Ensuring this protection may inadvertently sacrifice labor efficiency and incur additional costs related to sick leave, injury leave, or healthcare expenses, which would strongly incentivize automating the hazardous tasks.⁶

Overall, mapping these four occupational indices onto the commuting-zone-by-industry level, the results in Panel B consistently indicate that warming accelerates the substitution of labor with machines, supporting the concept of climate-induced automation. We test this directly in the next section.

Hot days vs. cold days. For cold days, we do not find interpretable sensitivities related to occupational temperature exposure. Similar to the results of the sectoral heterogeneity analysis in Section 3.1, the effects of cold days appear to be relatively uniform across sectors. We propose several speculative explanations. First, during extremely cold winters, workers in northern regions may be unable to operate outdoors under conditions of heavy snowfall. Second, outdoor workers in the construction or mining sectors are often required to wear personal protective equipment (PPE) for safety, such as helmets, gloves, and poorly ventilated clothes, making them more resilient to cold temperatures but vulnerable to heat. Third, regardless of occupation type, workers may be equally exposed to cold temperatures during commuting hours when daily temperatures are at their lowest, particularly in the morning.⁷ Even if commuters use cars or public transportation, commuting time may serve as a universal interface with cold weather for commuting employees, including those who work indoors in controlled environments.

⁵Injury and illness risk for each occupation is computed as the average incidence of working at least weekly under nine hazardous workplace conditions in the WCS, including exposure to Disease or Infections, Contaminants, Radiation, Minor Burns, Cuts, Bites, or Stings.

⁶Linking daily temperature data to universal daily injury records from Texas, [Park et al. \(2021\)](#) find that increased hot days lead to more occupational injuries.

⁷We calculate that the average commuter spends 55 minutes per day in a round trip, constituting 11.5% of typical daily working hours, using 2018–19 ACS data.

4.2 Climate-Induced Automation

This subsection directly investigates whether extreme temperatures have facilitated the adoption of labor-saving technologies, focusing specifically on industrial robots (hereafter referred to simply as robots). The growing literature on robots (Graetz and Michaels, 2018; Acemoglu and Restrepo, 2020, among others) commonly relies on data from IFR (2019), which defines a robot as “an automatically controlled, reprogrammable, and multipurpose machine.” Since IFR (2019) provides data only for 16 non-service industries in the US from 2004 onwards, we complement this with data from the National Income and Product Accounts (NIPA) by the BEA, which includes 54 four-digit NAICS industries over a longer period from 1947 to 2015. Using NIPA capital stocks and investments in Private Nonresidential Fixed Assets, we proxy robots as a combination of *metalworking machinery* and *special industrial machinery*, which we verify statistically aligns with the IFR data (see Appendix I.5). Due to missing data on robots in earlier periods, especially for non-manufacturing industries, we focus on 1980–2015, covering approximately equal durations of both the stable and declining phases of the labor share. As the datasets do not record robot usage at the regional level, we conduct an industry-level analysis instead. Specifically, for nonfarm, nonfinancial industry k during period I , we apply an industry-level analog of the baseline model (1):

$$\text{Robot}_{k,\bar{I}} = \beta^h \text{hd}_{k,I} + \beta^c \text{cd}_{k,I} + \mathbf{A}\mathbf{C}_{k,I} + \mathbf{F}\mathbf{Z}_{k,\underline{I}} + \mathbb{I}(\text{Division})\bar{I} + \delta_k + \delta_I + \varepsilon_{k,\bar{I}}, \quad (3)$$

where $\text{Robot}_{k,\bar{I}}$ represents various measures of robot adoption for industry k at the period end \bar{I} . Using county-level hot and cold day counts, $\text{hd}_{l,I}$ and $\text{cd}_{l,I}$, we construct a shift-share measure of industry k ’s exposure to hot and cold days during period I , $\text{hd}_{k,I}$ and $\text{cd}_{k,I}$, as follows:

$$\text{hd}_{k,I} = \sum_l \omega_{k,\underline{I}}^l \text{hd}_{l,I}, \quad \text{cd}_{k,I} = \sum_l \omega_{k,\underline{I}}^l \text{cd}_{l,I},$$

where $\omega_{k,\underline{I}}^l = L_{k,l,\underline{I}}/L_{k,\underline{I}}$ is county l ’s start-of-period employment share in industry k , computed from the CBP data (Eckert et al., 2021).⁸

We also control for other climate variables, $\mathbf{C}_{k,I}$, and socio-economic covariates, $\mathbf{Z}_{k,\underline{I}}$, computed analogously.⁹ The extended coverage provided by NIPA allows for a long-difference analysis over decade-long periods. For the IFR analyses, we use five-year intervals instead to ensure an adequate sample size. To control for trends in rising temperatures and accelerating automa-

⁸A conventional shift-share design interacts regional industry employment shares and industry exposure to some nationwide shocks to form a regional treatment variable (Goldsmith-Pinkham et al., 2020). In our industry-level analysis of robot adoption, we instead adopt a reverse shift-share design by interacting the spatial distribution of industries and regional exposure to extreme temperatures.

⁹We include a set of demographic compositions, industrial structure, and employment characteristics as controls. The detailed list of industry-level covariates is provided in Appendix II.3.

tion, we include division-level trends, $\mathbb{I}(\text{Division})\bar{I}$, in the regression, where divisions represent mining, utilities/construction, manufacturing, retail, transportation, and services. The model also includes two-way fixed effects δ_k and δ_I . Standard errors are clustered at the division level.

Panel A of Table 3 presents results using the BEA data. Column (1) examines the share of robots within total capital stock, revealing a significantly positive impact from both hot and cold days. This suggests that industries facing greater exposure to extreme temperatures systematically deploy more robots. Column (2) corroborates this pattern, showing a similarly positive effect on the share of robots within physical equipment. Column (3) examines robot investment as a share of total investment, showing that industries more exposed to hot and cold days allocate a larger portion of their capital investment to robots. Finally, Column (4) confirms a similarly augmenting effect on robot investment as a share of GDP. Overall, these findings suggest that industries more exposed to extreme temperatures exhibit a heightened reliance on automation.

As a placebo test, we repeat the analysis by replacing robots with general physical equipments, structures, and intellectual property products (IPP), respectively. None of these, in either stocks or investments, show significant responses (Table A-11). The pronounced impact of extreme temperature days on robots, together with the null effects on equipments and other forms of capital, suggests that the primary mechanism through which climate change reduces labor share is automation—by substituting labor with robots across an expanding range of tasks (Acemoglu and Restrepo, 2018)—rather than a general capital-labor substitution.¹⁰ Furthermore, to explore alternative modes of technological change, we examine the response of computer capital and software, a subset of equipment and IPP respectively, in a similar manner.¹¹ We find no evidence that climate change drives digitization (Table A-12), consistent with the observation that digitization mainly impacts white-collar workers and they mostly work indoors in controlled environments.

We further cross-validate the analyses using IFR data in Panel B of Table 3. Although the IFR data measure robots in units rather than in dollars, we obtain similar results, despite the more limited variation across industries and years. Overall, this section provides the evidence that higher exposure to extreme temperatures accelerates robot adoption, supporting our hypothesis of climate-induced automation.

Our findings also complement emerging studies on climate adaptation. Using the US Census of Manufacturers, Ponticelli et al. (2023) find that warming counties experience increased

¹⁰This is consistent with recent plant-level evidence provided by Oberfield and Raval (2021), who estimate the aggregate capital-labor elasticity of substitution to be less than one.

¹¹Computer capital consists of *PCs* and *mainframes*, while software consists of *prepackaged software*, *custom software*, and *own account software*. Aum and Shin (2024) explores the role of software in reducing the labor share.

Table 3: Climate and Robot Adoption Across Industries

Panel A: Industrial Robots from the BEA				
(units: percentage points)				
	Robot /Capital	Robot /Equipment	Robot Inv. /Capital Inv.	Robot Inv. /GDP
	(1)	(2)	(3)	(4)
10 hot days	2.740 (0.464)	5.770 (1.390)	4.830 (1.860)	1.170 (0.515)
10 cold days	3.810 (1.330)	4.720 (1.460)	7.560 (3.150)	1.450 (0.737)
climate variables	✓	✓	✓	✓
start-of-period controls	✓	✓	✓	✓
industry FE	Yes	Yes	Yes	Yes
year FE	Yes	Yes	Yes	Yes
division trend	Yes	Yes	Yes	Yes
Observations	200	200	200	200
Adjusted R ²	0.965	0.956	0.939	0.846
Panel B: Industrial Robots from the IFR				
(units: robots/100 million USD)				
	(1)	(2)	(3)	(4)
10 hot days	3.990 (0.708)	11.10 (1.720)	18.20 (2.420)	1.300 (0.336)
10 cold days	4.810 (1.260)	12.00 (2.600)	25.50 (3.330)	2.030 (0.192)
climate variables	✓	✓	✓	✓
start-of-period controls	✓	✓	✓	✓
industry FE	Yes	Yes	Yes	Yes
year FE	Yes	Yes	Yes	Yes
division trend	Yes	Yes	Yes	Yes
Observations	51	51	51	68
Adjusted R ²	0.988	0.976	0.682	0.934

Notes: The thresholds for hot and cold days are set analogously at 77°F and 50°F, respectively. We focus on nonfarm, nonfinancial industries. All regressions are weighted by industry GDP. Standard errors in parentheses are clustered at the division level. See main text and Appendix II.3 for more details. (Panel A) Unit of analysis: outcome years (1980–2010 by decades) \times industries. (Panel B) Unit of analysis: outcome years (2005, 2010, 2015, 2019) \times industries.

concentration of production in large plants through the downsizing or closure of small plants. Acharya et al. (2023) show that multi-establishment firms respond to warming by reallocating employment from plants in affected counties to unaffected ones. Our study highlights robot adoption as an overlooked facet of climate adaptation strategies.

5 Assessment of Macroeconomic Impacts

Armed with our estimates, we quantitatively assess the impact of climate change on the dynamics of the labor share. Guided by Figure 1a, we separately study a period of stable labor share (1950–2001) and a period of declining labor share (2001–2019). Figure 2a presents a histogram of climate exposure across counties, with red bars representing changes in the decadal average number of hot days and blue bars representing changes in cold days. Between 1950 and 2001, the (employment-weighted) median county experienced 9.0 more hot days and 4.7 fewer cold days. In contrast, from 2001 to 2019, the increase in hot days was predominant, with the median county experiencing 12.5 more hot days and only 1.2 fewer cold days.

We compute the aggregate impact of climate change on labor share $\Delta\text{LaborShare}$ from year t_0 to t_1 as

$$\Delta\text{LaborShare} = \underbrace{\sum_l \omega^l \beta^h (\text{hd}_{l,t_1} - \text{hd}_{l,t_0})}_{\text{effect from hot days}} + \underbrace{\sum_l \omega^l \beta^c (\text{cd}_{l,t_1} - \text{cd}_{l,t_0})}_{\text{effect from cold days}}, \quad (4)$$

where ω^l is the GDP share of county l in 2001. The terms $\text{hd}_{l,t}$ and $\text{cd}_{l,t}$ denote decadal averages of hot and cold days, respectively.¹² In addition, we also compute the implied impacts separately for each sector, using the sector-specific estimates for construction/mining, manufacturing, low-skilled services (e.g., transportation, retail, healthcare, restaurants), and high-skilled services, as reported in Appendix II.2. We then apply the estimates into a similar formula to Equation (4) for each sector (see Appendix II.4).

Figure 2b reports implied impacts on the nationwide labor share, both overall and by sector, separately for 1950–2001 and 2001–2019. Extrapolating sector-specific estimates back to the previous century, we find that the adverse effect from the increase in hot days (+9.0 days) has been largely offset by the decrease in cold days (−4.7 days) (Panel (b), left).¹³ In contrast, from 2001 to 2019, the pronounced increase in hot days dramatically outweighs the decrease in cold days. Our calculations indicate that climate change accounts for 13.7% of the overall

¹²Our estimates capture within-cell changes. A within-between decomposition reveals that the within component nearly equals the overall decline in labor share during 2001–2019.

¹³Since estimates from county-by-industry labor share data for 1950–2001 are unavailable, we run a counterfactual simulation presuming that the elasticities are consistent across both periods.

observed declining trend in labor share during this period.¹⁴ Overall, the pattern of climate change aligns well with both the stability and subsequent decline of labor share. We conduct several robustness checks with alternative models in Appendix II.4, and our assessments remain similar.

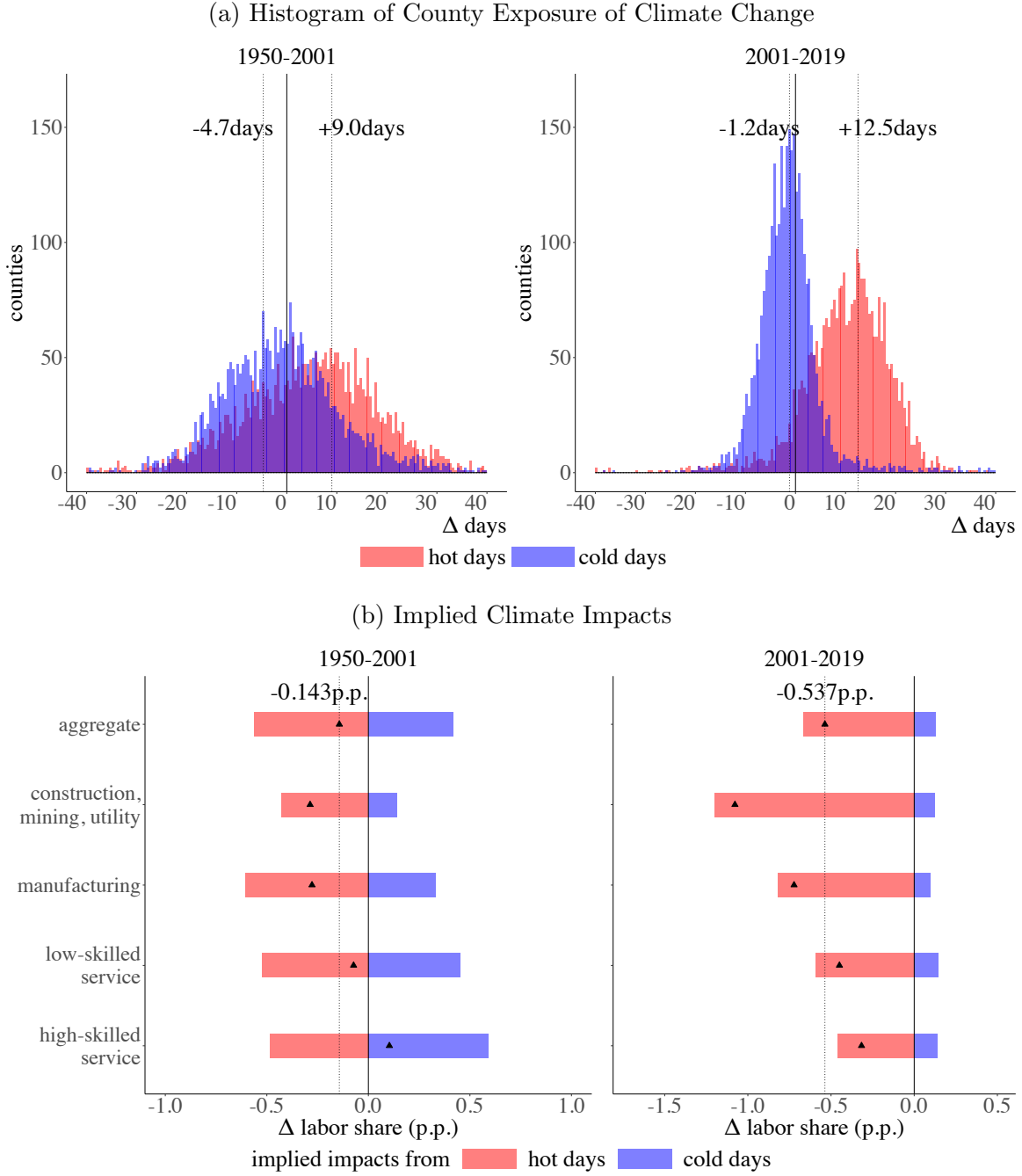
Our findings contribute to a joint explanation for both the stability of labor share in earlier decades and its subsequent decline. To account for the past constancy of labor share, [Acemoglu and Restrepo \(2018\)](#) introduce the creation of new tasks as a counterbalancing force to automation that reduces labor share. [Hubmer \(2023\)](#) posits that post-war economic growth increases labor share through an income effect, as higher-income households tend to consumer more labor-intensive goods. Our climate-based perspective demonstrates that the positive impacts of a decrease in the number of cold days offset the negative impacts of an increase in the number of hot days in the last century.

6 Conclusion

The 21st century has witnessed an unprecedented decline in the labor share, alongside a concerning rise in global temperatures. This paper connects these two phenomena through the lens of endogenous technological change. Using granular county-level exposure to extreme daily weather in the US as a natural experiment, we provide a coherent long-run picture that climate change has affected labor share dynamics, accounting for 14% of the observed decline in the US labor share after 2000 while maintaining a stable labor share in the last century. Our findings suggest that climate change has propelled automation, and contributed to a widening inequality of the wealth of the nation. This study contributes to the recent debate on the decline of labor share, and the burgeoning inquiry into the macroeconomic impacts of climate change.

¹⁴To isolate cyclical effects, we calculate the decline in the aggregate labor share as a decrease in its linear trend (-3.92 p.p.), using the same county-level data used in the estimation for internal consistency. The raw decline in the labor share is -4.80 p.p., with climate change estimated to account for 11.2% of this decline.

Figure 2: Implied Impacts of Climate Change on Labor Share (1950-2001 vs. 2001-2019)



References

- Acemoglu, Daron**, “Directed Technical Change,” *The Review of Economic Studies*, 2002, *69* (4), 781–809.
- **and Pascual Restrepo**, “The Race between Man and Machine: Implications of Technology for Growth, Factor Shares, and Employment,” *American Economic Review*, 2018, *108* (6), 1488–1542.
- **and —**, “Automation and New Tasks: How Technology Displaces and Reinstates Labor,” *Journal of Economic Perspectives*, 2019, *33* (2), 3–30.
- **and —**, “Robots and Jobs: Evidence from US Labor Markets,” *Journal of Political Economy*, 2020, *128* (6), 2188–2244.
- **and —**, “Demographics and Automation,” *The Review of Economic Studies*, 2022, *89* (1), 1–44.
- Acharya, Viral V, Abhishek Bhardwaj, and Tuomas Tomunen**, “Do Firms Mitigate Climate Impact on Employment? Evidence from US Heat Shocks,” Working Paper 31967, National Bureau of Economic Research December 2023.
- Aum, Sangmin and Yongseok Shin**, “Is Software Eating the World?,” Working Paper 32591, National Bureau of Economic Research June 2024.
- Autor, David, David Dorn, Lawrence F Katz, Christina Patterson, and John Van Reenen**, “The Fall of the Labor Share and the Rise of Superstar Firms,” *The Quarterly Journal of Economics*, 2020, *135* (2), 645–709.
- Autor, David H and David Dorn**, “The Growth of Low-skill Service Jobs and the Polarization of the US Labor Market,” *American Economic Review*, 2013, *103* (5), 1553–1597.
- **, Frank Levy, and Richard J Murnane**, “The Skill Content of Recent Technological Change: An Empirical Exploration,” *The Quarterly Journal of Economics*, 2003, *118* (4), 1279–1333.
- Barreca, Alan, Karen Clay, Olivier Deschenes, Michael Greenstone, and Joseph S Shapiro**, “Adapting to Climate Change: The Remarkable Decline in the US Temperature-mortality relationship over the Twentieth Century,” *Journal of Political Economy*, 2016, *124* (1), 105–159.
- Cachon, Gerard P, Santiago Gallino, and Marcelo Olivares**, “Severe Weather and Automobile Assembly Productivity,” Technical Report 2012.

- Chen, Xiaoguang and Lu Yang**, “Temperature and Industrial Output: Firm-level Evidence from China,” *Journal of Environmental Economics and Management*, 2019, *95*, 257–274.
- Colmer, Jonathan**, “Temperature, Labor Reallocation, and Industrial Production: Evidence from India,” *American Economic Journal: Applied Economics*, 2021, *13* (4), 101–124.
- De Loecker, Jan, Jan Eeckhout, and Gabriel Unger**, “The Rise of Market Power and the Macroeconomic Implications,” *The Quarterly Journal of Economics*, 2020, *135* (2), 561–644.
- Dell, Melissa, Benjamin F Jones, and Benjamin A Olken**, “Temperature Shocks and Economic Growth: Evidence from the Last Half Century,” *American Economic Journal: Macroeconomics*, 2012, *4* (3), 66–95.
- Deryugina, Tatyana and Solomon M Hsiang**, “Does the Environment Still Matter? Daily Temperature and Income in the United States,” Technical Report, National Bureau of Economic Research 2014.
- Eckert, Fabian, Peter K. Fort, Teresa C. and Schott, and Natalie J. Yang**, “Imputing Missing Values in the US Census Bureau’s County Business Patterns,” *NBER Working Paper*, 2021, *26632*.
- Elsby, Michael WL, Bart Hobijn, and Aysegül Şahin**, “The Decline of the US Labor Share,” *Brookings Papers on Economic Activity*, 2013, *2013* (2), 1–63.
- Giandrea, Michael D and Shawn A Sprague**, “Estimating the US Labor Share,” *Monthly Labor Review*, 2017.
- Goldsmith-Pinkham, Paul, Isaac Sorkin, and Henry Swift**, “Bartik Instruments: What, When, Why, and How,” *American Economic Review*, 2020, *110* (8), 2586–2624.
- Graetz, Georg and Guy Michaels**, “Robots at Work,” *Review of Economics and Statistics*, 2018, *100* (5), 753–768.
- Grossman, Gene M and Ezra Oberfield**, “The Elusive Explanation for the Declining Labor Share,” *Annual Review of Economics*, 2022, *14* (1), 93–124.
- Gutiérrez, Germán and Sophie Piton**, “Revisiting the Global Decline of the (Non-housing) Labor Share,” *American Economic Review: Insights*, 2020, *2* (3), 321–338.
- Hubmer, Joachim**, “The Race Between Preferences and Technology,” *Econometrica*, 2023, *91* (1), 227–261.
- IFR**, “World Robotics: Industrial Robots,” Technical Report 2019.

- Kaldor, Nicholas**, “Capital Accumulation and Economic Growth,” in “The Theory of Capital: Proceedings of a Conference Held by the International Economic Association” Springer 1961, pp. 177–222.
- Karabarbounis, Loukas and Brent Neiman**, “The Global Decline of the Labor Share,” *The Quarterly Journal of Economics*, 2014, 129 (1), 61–103.
- Kehrig, Matthias and Nicolas Vincent**, “The Micro-Level Anatomy of the Labor Share Decline,” *The Quarterly Journal of Economics*, 2021, 136 (2), 1031–1087.
- Koh, Dongya, Raül Santaeulàlia-Llopis, and Yu Zheng**, “Labor Share Decline and Intellectual Property Products Capital,” *Econometrica*, 2020, 88 (6), 2609–2628.
- Kravis, Irving B**, “Relative Income Shares in Fact and Theory,” *The American Economic Review*, 1959, 49 (5), 917–949.
- Lewis, Ethan**, “Immigration, Skill Mix, and Capital Skill Complementarity,” *The Quarterly Journal of Economics*, 2011, 126 (2), 1029–1069.
- Moscona, Jacob and Karthik A Sastry**, “Does Directed Innovation Mitigate Climate Damage? Evidence from U.S. Agriculture,” *The Quarterly Journal of Economics*, 10 2022, 138 (2), 637–701.
- Nath, Ishan B, Valerie A Ramey, and Peter J Klenow**, “How Much Will Global Warming Cool Global Growth?,” Working Paper 32761, National Bureau of Economic Research 2024.
- Oberfield, Ezra and Devesh Raval**, “Micro Data and Macro Technology,” *Econometrica*, 2021, 89 (2), 703–732.
- Park, Jisung, Nora Pankratz, and Arnold Behrer**, “Temperature, Workplace Safety, and Labor Market Inequality,” Technical Report 2021.
- Peri, Giovanni and Akira Sasahara**, “The Impact of Global Warming on Rural-Urban Migrations: Evidence from Global Big Data,” Technical Report, National Bureau of Economic Research 2019.
- **and Chad Sparber**, “Task Specialization, Immigration, and Wages,” *American Economic Journal: Applied Economics*, 2009, 1 (3), 135–169.
- Ponticelli, Jacopo, Qiping Xu, and Stefan Zeume**, “Temperature and Local Industry Concentration,” Working Paper 31533, National Bureau of Economic Research August 2023.
- Presidente, Giorgio**, “Labor Services At Will: Regulation of Dismissal and Investment in Industrial Robots,” *mimeo*, 2017.

- Rognlie, Matthew**, “Deciphering the Fall and Rise in the Net Capital Share: Accumulation or Scarcity?,” *Brookings Papers on Economic Activity*, 2015, *2015* (1), 1–69.
- Somanathan, Eswaran, Rohini Somanathan, Anant Sudarshan, and Meenu Tewari**, “The Impact of Temperature on Productivity and Labor Supply: Evidence from Indian Manufacturing,” *Journal of Political Economy*, 2021, *129* (6), 1797–1827.
- Tolbert, Charles M and Molly Sizer**, “U.S. Commuting Zones and Labor Market Areas: A 1990 Update,” Technical Report 1996.
- Webb, Michael**, “The Impact of Artificial Intelligence on the Labor Market,” *Available at SSRN 3482150*, 2019.
- Zivin, Joshua Graff and Matthew Neidell**, “Temperature and the Allocation of Time: Implications for Climate Change,” *Journal of Labor Economics*, 2014, *32* (1), 1–26.

APPENDICES FOR ONLINE PUBLICATION

Climate Change and the Decline of Labor Share

Xincheng Qiu and Masahiro Yoshida

November 19, 2024

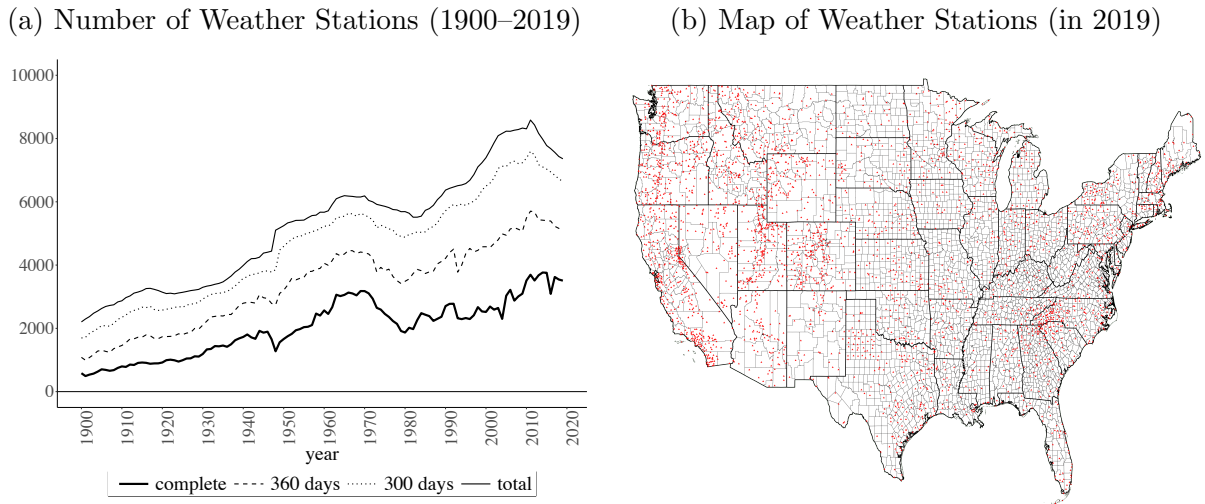
I Additional Data Details

I.1 Climate Data

Weather stations. The left panel of Figure A-1 shows the long-run trend in the number of weather stations operating in the US from 1900 to 2019. It plots four lines based on the completeness of stations' daily records each year, including the number of stations with complete daily records, with at least 360 days of records per year, with at least 300 days of records per year, as well as the total number of weather stations. The number of stations in operation generally increases over time.

The right panel of Figure A-1 depicts the geographic distribution of stations with complete records in 2019. Each dot represents a weather station, and the boundaries mark county borders. The map shows dense climate monitoring overall, particularly at populous areas along the East and West Coast and in the Midwest, although the less-populous mountainous regions have somewhat sparser coverage of weather stations.

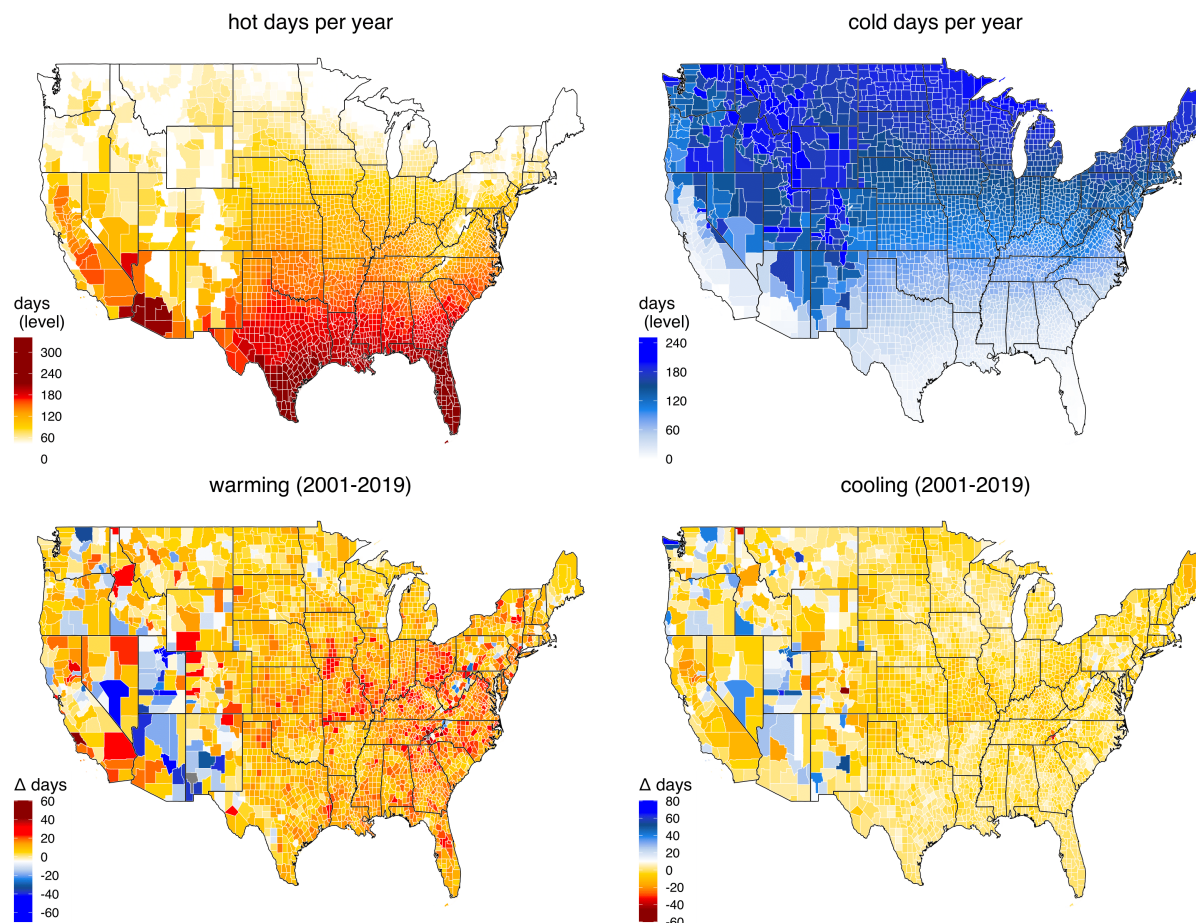
Figure A-1: Weather Stations in the US Mainland



Notes: Panel (a) plots the number of weather stations in the US mainland from the Global Historical Climatology Network Daily (GHCN-daily), provided by the National Climatic Data Center (NCDC) of the National Oceanic and Atmospheric Administration (NOAA). Panel (b) plots the geographic distribution of weather stations (red triangles), where county and state borders are depicted by thin and thick lines, respectively.

Spatial distribution of hot and cold days. Daily records, such as minimum and maximum temperature, precipitation, and snowfall, from 3 weather stations closest to county population centroids in 2020 are aggregated using an inverse-distance weighting method. Population centroids of US counties are available from the [Census Bureau](#).

Figure A-2: Hot and Cold Days across US Counties

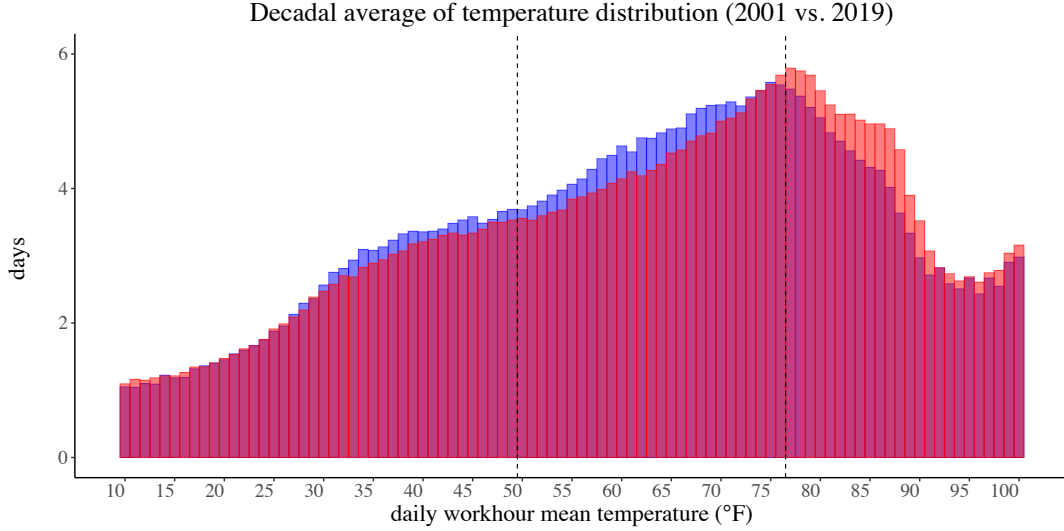


Notes: Top Panel: level in 2019; Bottom Panel: change from 2001 to 2019. Thresholds for hot and cold days are set to 77°F and 50°F based on the average temperature during working hours (8 a.m.–6 p.m.), with a weighting factor of 0.75 applied to the daily maximum temperature. The decadal averages of annual hot and cold days are calculated for the periods 1992–2001 to represent the year 2001, and 2010–2019 to represent the year 2019.

Figure A-2 displays the geographic distribution of hot and cold days across counties. The top pattern shows the annual levels of hot days (left) and cold (right) days in 2019, and the bottom panel depicts the change in the frequency of hot (left) and cold (right) days from 2001 to 2019. Although, not surprisingly, hot days are more concentrated in the south and cold days are more concentrated in the north, the patterns of “warming” (i.e., changes in the number of hot days) and “cooling” (i.e., changes in the number of cold days) are more geographically dispersed across the country.

Distribution of climate exposure. Figure A-3 illustrates the distributions of the decadal average working hour temperature in 2001 vs. 2019. Each bar represents the annual number of days with work hour temperatures falling into each 1°F-bin, weighted by employment at the

Figure A-3: Exposure to Climate Change in the US



Notes: Blue: 2001 (1992–2001); Red: 2019 (2010–2019). Each histogram illustrates nationwide climate exposure across each 1°F bin, which is aggregated of the annual number of days with county-level working hour (8 a.m.–6 p.m.) temperature falling into each bin. In the periods of 1992–2001 and 2010–2019, aggregation weights are based on start-of-period employment levels from 1992 and 2010, respectively. The sum of days are normalized to 365 days. The dotted lines show our baseline thresholds for hot and cold days, 77°F and 50°F.

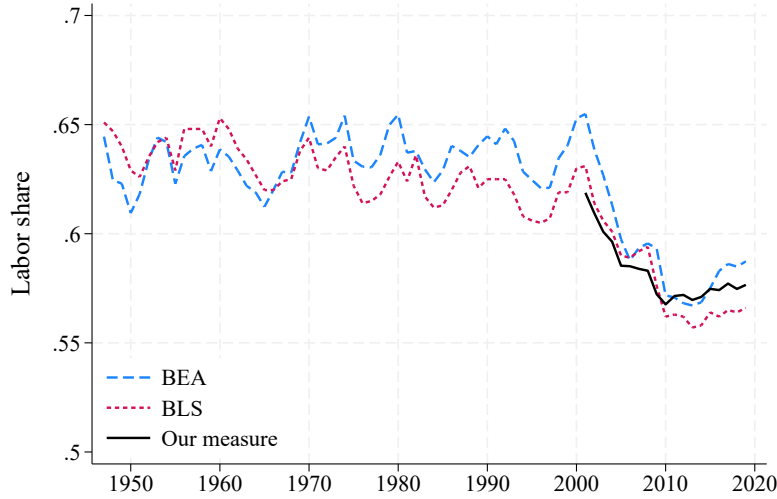
start of each period. The figure depicts a noticeable shift in average temperature distribution to the right, with a higher concentration of days in higher temperature bins in 2019 compared to the 2001, highlighting the warming trend. The dashed lines mark the cutoffs used in the baseline analysis to define hot and cold days, 77°F and 50°F, aligned with the thresholds for the top and bottom terciles, respectively, in the latest decade, 2010–2019.

I.2 Labor Share

Comparison to official statistics. The Bureau of Labor Statistics (BLS) headline labor share measure assumes equal wages for the self-employed and payroll-employed, and imputes proprietors’ labor income by multiplying proprietors’ hours by employees’ hourly compensation (Giandrea and Sprague, 2017). This approach is referred to as the “labor basis” measure by Kravis (1959). However, this imputation is impractical at the county level due to the lack of data on proprietors’ hours. The BLS labor share covers the nonfarm business sector and is the most commonly used series, while the Bureau of Economic Analysis (BEA) measure, instead, focuses on the nonfinancial corporate sector, thereby avoiding ambiguities related to the classification of proprietors’ income as labor or capital income.

We aggregate our labor share measure at the county level to the national level, and compare

Figure A-4: Alternative Measures of the Labor Share



Notes: This figure compares our measure of labor share aggregated to the national level with the official measures by the BEA and the BLS.

it with the official measures of the national labor share by both the BLS and the BEA in Figure A-4. Our measure, though only available after 2001, aligns closely with the BEA and BLS series during the overlapping period. Notably, our measure captures a similar decline in the labor share. The consistency with both official series reassures the reliability of our measure.

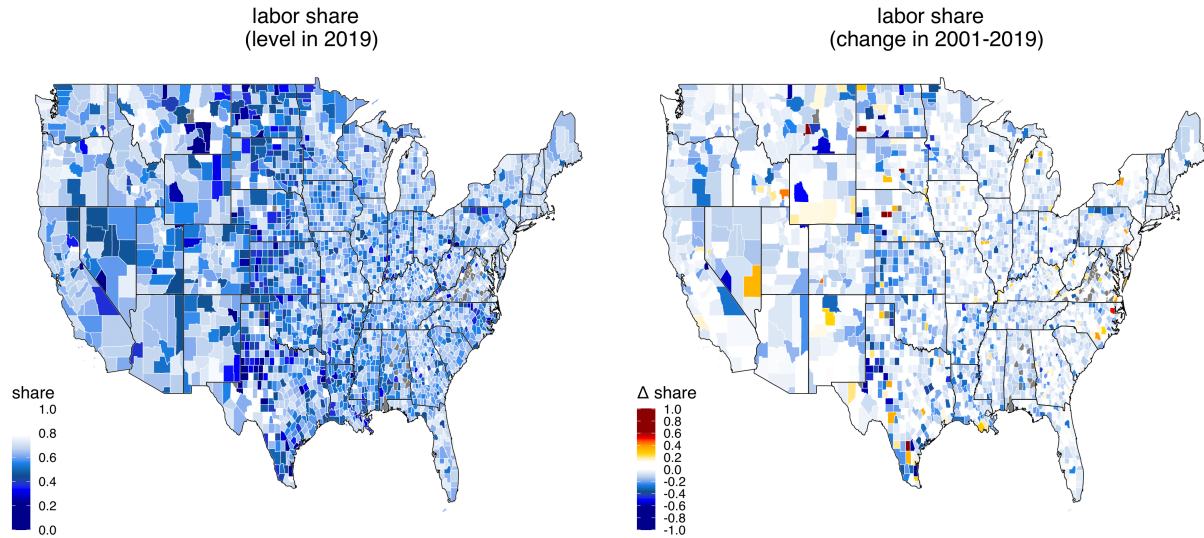
Linking data. We merge local climate data with local labor share data based on county FIPS codes. Note that the BEA Regional Economic Accounts record local economic activities in Virginia as 23 combination areas (FIPS 51901–51958), to which we manually merge the 51 Virginia counties (FIPS 51003–51735). The dataset comprises a panel of 3,080 counties in the US mainland. Due to missing data, four small counties with populations below 1,000—Petroleum, MT (FIPS 30069), Loup, NE (FIPS 31115), Loving, TX (FIPS 48301), and Roberts, TX (FIPS 48393)—are dropped, resulting in 3,076 counties in the analysis.

The 16 NAICS-based industries in the BEA data contain 21 (mining, quarrying, and oil and gas extraction), 22 (utilities), 23 (construction), 31–33 (manufacturing), 42 (wholesale trade), 44–45 (retail trade), 48–49 (transportation and warehousing), 51 (information), 54 (professional, scientific, and technical services), 55 (management of companies and enterprises), 56 (administrative and support and waste management and remediation services), 61 (educational services), 62 (health care and social assistance), 71 (arts, entertainment, and recreation), 72 (accommodation and food services), 81 (other services). We use nonfarm, nonfinancial private industries; 11 (agriculture, forestry, fishing and hunting), 52 (finance and insurance), 53 (real estate and rental and leasing), and 92 (public administration) are excluded. We drop county-

by-industry observations with missing labor share. Moreover, we restrict our analysis to cells with labor shares falling within the range $(0, 1)$.

Heat map. Figure A-5 depicts the labor share across counties in 2019 (left) and the change in labor share between 2001 and 2019 (right). It reveals significant spatial variation in both the level and the change in labor share. The decline in the labor share is prevalent, as is evident from the right panel.

Figure A-5: Labor Shares across US Counties



Notes: Labor share is calculated as the ratio of wage compensation divided by GDP excluding proprietors' income obtained from the BEA Regional Economic Accounts. Bold lines are state borders.

Summary statistics. Table A-1 presents the summary statistics for the sample used in our baseline analysis. For each outcome year (2001, 2010 and 2019), the decadal averages of the number of hot and cold days are calculated at the county level, while labor shares are measured at the county-by-industry level. Over the study period, the median county experiences 86.7 hot days and 111.2 cold days annually, roughly equivalent to 3 and 3.5 months per year, respectively.

Statewide relationship. Figure A-6 shows the relationship between the decadal average number of hot days per year and the average labor share across US states in 2019. Each circle corresponds to a state, with the size of each bubble representing the denominator of labor share (i.e., GDP minus proprietors' income). One can see that states with exposed to more hot days typically have a lower labor share. This negative correlation between hot days and labor share, indicated by the downward-sloping GDP-weighted fitted line, is significant, with an estimated slope of -0.025 and a standard error of 0.01 .

Table A-1: Summary Statistics

	Mean	SD	P10	P25	Median	P75	P90	Obs
Panel A: county level by year								
hot days	90.8	49.6	29.0	50.3	86.7	126.6	158.7	9,228
cold days	106.5	53.9	28.2	61.6	111.2	150.9	174.9	9,228
Panel B: county-industry level by year								
labor share	0.673	0.204	0.396	0.554	0.685	0.828	0.923	93,452

Notes: This table reports unweighted summary statistics for the key variables in our baseline analysis. Unit of statistics for hot and cold days: outcome years (2001, 2010, 2019) \times counties; Unit of statistics for labor shares: outcome years \times counties \times industries.

I.3 Covariates

Extra climate variables. In addition to hot and cold days, we include the period I 's average of daily precipitation on rainy days (intensive margin), the number of non-rainy days (extensive margin), and the number of days with heavy snowfall (≥ 300 mm).

Demography. The first group contains the start-of-period I 's demographic variables of employment, a vector of employment shares by:

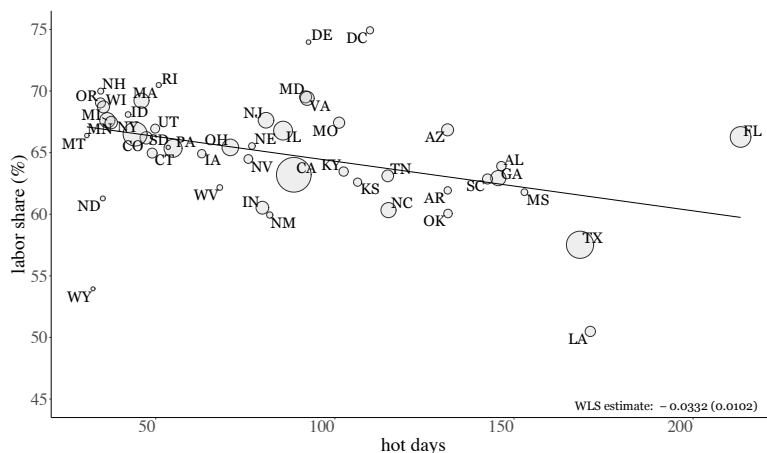
- education attainment: less than high school degrees, high school graduates, college graduates, above college degrees ("some college years" is omitted as a benchmark)
- age bins: 16–24, 25–34, 35–44, 45–54, 55–64 ("65 and above" is omitted as a benchmark)
- race and ethnicity: non-hispanic whites, non-hispanic blacks, hispanics ("non-hispanic asians" and "other races" are omitted as a benchmark)
- other demographics: immigration status (foreign-born, non-citizens), gender, veteran status

These variables are constructed at the level of 16 industries by 722 commuting zones using data from the 1990 and 2000 Census and the 2009–2010 stacked American Community Survey.

Industry structure. To capture market structure dynamics that could influence the labor share, the second group includes the start-of-period I 's measures of industry structure:

- Herfindahl-Hirschman Index (HHI)
- employment share of large establishments with over 1,000 employees

Figure A-6: Hot Days and Labor Shares across US States (2019)



Notes: This figure presents a scatterplot of the statewide labor share against the prior decade average of hot days per year across US states in 2019. Hot days are 2010 employment-weighted average of hot days (with working-hour temperature above 77°F) during 2010–2019 across counties. The bubble size captures the denominator of labor share (i.e., GDP minus proprietors' income) in 2019.

These variables are constructed at the level of 16 industries by 3,080 counties, using the County Business Pattern data in 1990, 2000, 2010.

Labor market variables. The third group includes the start-of-period I 's regional labor market variables:

- per capita non-labor income and welfare income
- population share of those who rent a house
- unemployment ratio of population
- log of population density

These variables are constructed at the level of 722 commuting zones, using data from the 1990 and 2000 Census, and the 2009–2010 stacked American Community Survey.

I.4 Occupation Characteristics

Physical intensity We borrow the occupation-level physical intensity from [Peri and Sparber \(2009\)](#). The index is the average of the following variables of O*NET Ability Survey:

- **Limb, hand, and finger dexterity**
 - 1.A.2.a.1: arm-hand steadiness
 - 1.A.2.a.2: manual dexterity

- 1.A.2.a.3: finger dexterity
- 1.A.2.b.1: control precision
- 1.A.2.b.4: rate control
- 1.A.2.c.1: reaction time
- 1.A.2.c.2: wrist-finger speed
- 1.A.2.c.3: speed of limb movement
- **Body coordination and flexibility**
 - 1.A.3.c.1: extent flexibility
 - 1.A.3.c.2: dynamic flexibility
 - 1.A.3.c.3: gross body coordination
 - 1.A.3.c.4: gross body equilibrium
- **Strength**
 - 1.A.3.a.1: static strength
 - 1.A.3.a.2: explosive strength
 - 1.A.3.a.3: dynamic strength
 - 1.A.3.a.4: trunk strength
 - 1.A.3.b.1: stamina

As noted in [Peri and Sparber \(2009\)](#), even when sensory-perception skills are included, comprising General perception, Visual perception, and Hearing perception, the results remain unchanged.

Manual routine intensity. Following [Autor et al. \(2003\)](#) and [Autor and Dorn \(2013\)](#), we use occupational task requirements from the fourth edition of the US Department of Labor’s Dictionary of Occupational Titles (DOT) to measure the routine, abstract, and manual task content for each occupation. The data can be downloaded from [David Dorn’s website](#). Tasks are rated on a scale from zero to ten. We compute manual routine intensity as $\log(\text{Routine}) + \log(\text{Manual})$.

Technological exposure to robots. [Webb \(2019\)](#) develops a new method to measure occupational exposure to automation by the overlap between the text of relevant patents, which describes technological capabilities, and the text of job descriptions, which describes tasks to be done by workers. He uses natural language processing to extract verbs from both sources. Data on each occupation’s exposure to robots, software and AI can be downloaded from [Michael Webb’s website](#).

Injury and illness risk. We compute for each occupation the fraction of employees working at least weakly under nine hazardous places at Work Context Survey, using questions 4.C.2.b.1.c–4.C.2.c.1.f.

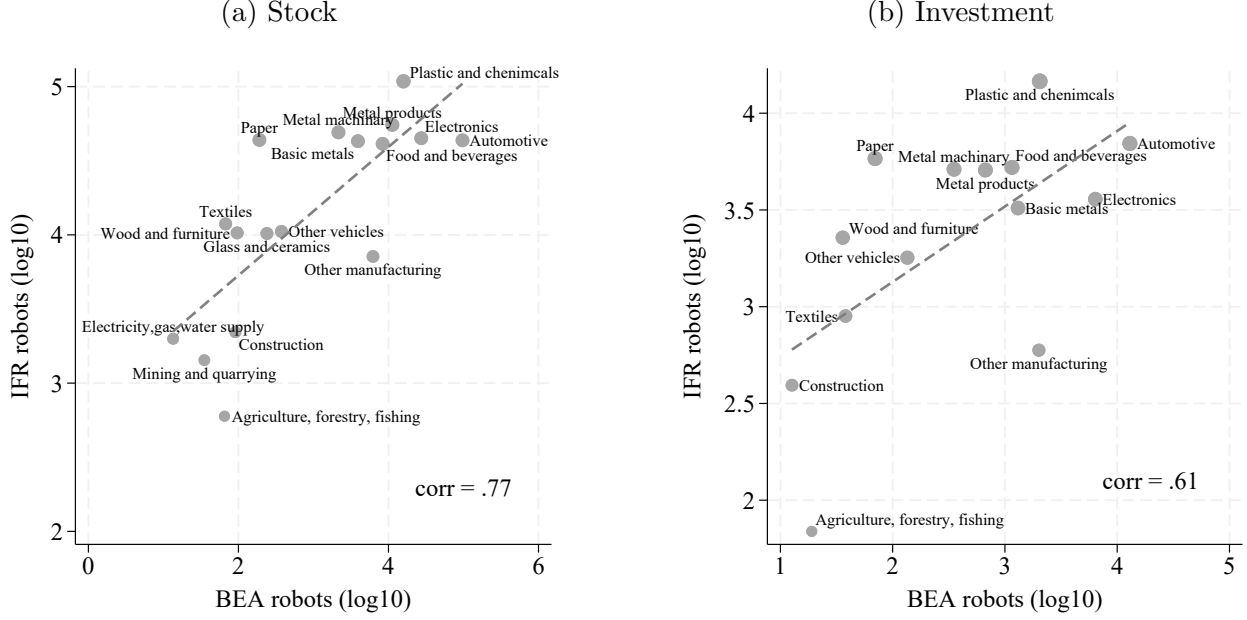
- **Frequency in Environmental Conditions:** “How often during a usual work period is the worker exposed to the following conditions?”
 - 4.C.2.b.1.c: Extremely Bright or Inadequate Lighting
 - 4.C.2.b.1.d: Exposed to Contaminants
 - 4.C.2.b.1.f: Exposed to Whole Body Vibration
- **Job Hazards:** “How often does this job require the worker to be exposed to the following hazards?”
 - 4.C.2.c.1.a: Exposed to Radiation
 - 4.C.2.c.1.b: Exposed to Disease or Infections
 - 4.C.2.c.1.c: Exposed to High Places
 - 4.C.2.c.1.d: Exposed to Hazardous Conditions
 - 4.C.2.c.1.e: Exposed to Hazardous Equipment
 - 4.C.2.c.1.f: Exposed to Minor Burns, Cuts, Bites, or Stings

I.5 Industrial Robots

Figure A-7 validates the BEA robot measure, a combination of *metalworking machinery* and *special industrial machinery*, by comparing it with the IFR robot measure in terms of both stock and investment. Following Graetz and Michaels (2018), we use the perpetual inventory method to estimate robot stocks, applying a depreciation rate of 10%, given the initial value of stock measure in 2004 provided by the IFR. This approach mirrors the EUKLEMS procedure for computing the stock of ICT capital. Our findings are robust to alternative depreciation rates of 5% or 15%, or directly using the IFR-reported stocks.

Panel (a) of Figure A-7 plots the BEA robot stock (in million USD) against the IFR robot stock (in units), revealing a strong positive correlation of 0.77. This indicates that the BEA measure we construct aligns well with the established IFR robot data. The close clustering of industries along the fitted line further supports the reliability of the BEA robot stock measure we construct as a proxy for robot deployment. Panel (b) compares the BEA robot investment measure (in million USD) with the IFR robot investment measure (in units), showing a positive correlation of 0.61, which again underscores their alignment. Overall, both panels ensure the reliability of the BEA proxy for capturing robotization trends in the US.

Figure A-7: Measurement: BEA Robots vs. IFR Robots



Notes: This figure compares the BEA robot measure (in million USD) with the IFR robot measure (in units) in terms of both stock (a) and investment (b). The dashed lines represent the fitted lines, with correlation of 0.77 and 0.61 for stock and investment, respectively. The size of each bubble captures log10 of BEA robots.

II Additional Analyses

II.1 Robustness Checks

This subsection presents a series of robustness checks to validate the paper's main findings.

Temperature thresholds. Table A-2 evaluates the robustness of our results to different temperature cutoffs. Specifically, we examine how varying the cutoffs for hot days at 73, 75, 77, 80°F, and for cold days at 35, 40, 45, 50, 55°F, affects the estimated impacts on labor share. Columns (1) through (4) report results for hot days defined by progressively higher temperature cutoffs, and Columns (5) through (8) report results for cold days defined by progressively lower temperature cutoffs. The results remain broadly consistent across different specifications with alternative cutoff pairs. However, the coefficients for hot days above 80°F in Column (4), as well as for cold days below 45°F, are estimated with less precision. This is likely due to limited statistical power arising from the relative rarity of these extremely-high temperature events. See the nonlinear temperature effects using more granular temperature bins below for more details.

Table A-2: By Temperature Thresholds

	dependent variable: labor share (units: percentage points)							
	Baseline							
	(1)	(2)	(3)	(4)	(5)	(6)	(7)	(8)
10 hot days $\geq 73^\circ\text{F}$	-0.627 (0.166)							
$\geq 75^\circ\text{F}$		-0.576 (0.157)						
$\geq 77^\circ\text{F}$			-0.589 (0.202)		-0.528 (0.206)	-0.433 (0.252)	-0.384 (0.256)	-0.433 (0.208)
$\geq 80^\circ\text{F}$				-0.334 (0.353)				
10 cold days $< 50^\circ\text{F}$	-0.910 (0.390)	-0.886 (0.395)	-0.874 (0.414)	-0.727 (0.515)				
$< 55^\circ\text{F}$					-0.634 (0.242)			
$< 45^\circ\text{F}$						-0.403 (0.406)		
$< 40^\circ\text{F}$							-0.232 (0.411)	
$< 35^\circ\text{F}$								-0.581 (0.556)
Observations	90,311	90,311	90,311	90,311	90,311	90,311	90,311	90,311
Adjusted R^2	0.815	0.815	0.815	0.815	0.815	0.815	0.815	0.815

Notes: Unit of analysis: outcome years (2001, 2010, 2019) \times counties \times industries. All models inherit the full controls and county, state-year, industry-year fixed effects at specification (5) from Table 1. The regressions are weighted by the denominator of labor share, i.e., GDP minus proprietors' income. Standard errors in parentheses are clustered at the state level.

Treatment window. Table A-3 reports the results of robustness checks using different treatment windows (1, 5, 10, 15, and 20 years). To compare models with alternative treatment windows, we create other climate variables \mathbf{C}_t averaged for each time window. Since socioeconomic controls are only available in Census years before 2000, we reassign pre-treatment full controls $\mathbf{Z}_{t,k}$ as follows: for each outcome year 2001, 2010, 2019, controls are reconstructed at 1980, 1990, 2000 for 20 year windows, 1980, 1990, 2005 for 15 year windows, 1990, 2005, 2014 for 5 year windows and 1990, 2005 and 2014, for 1 year windows. For year 2005 and 2014, we use the two-year stacked ACS data in 2005–2006 and 2013–2014, respectively. The estimates remain broadly consistent across all specifications in Columns (1)–(5). However, they are weaker for shorter treatment windows (1 year and 5 years) and become stronger as the treatment window lengthens (10, 15, and 20 years).

Recall that Table 1 demonstrates that the inclusion of controls does not affect the estimates in terms of magnitude or precision. As a robustness check, in Column (6)–(10), we repeat

the analysis without including any controls. Once again, we find similar results, with longer treatment windows yielding stronger estimates. Shorter treatment windows produce estimates with the same signs but weaker magnitudes. We thus conclude that long-term climate change, rather than temporary weather shocks, is driving the changes in labor shares. This is consistent with the theory that technological change and capital adjustments take place over the long run.

Table A-3: By Treatment Window

dependent variable: labor share					
(units: percentage points)					
	1 year	5 year	10 year	15 year	20 year
			baseline		
	(1)	(2)	(3)	(4)	(5)
10 hot days	-0.082 (0.138)	0.015 (0.135)	-0.589 (0.202)	-0.646 (0.307)	-0.917 (0.437)
10 cold days	-0.230 (0.170)	-0.518 (0.139)	-0.874 (0.414)	-1.400 (0.964)	-1.950 (0.871)
climate variables	✓	✓	✓	✓	✓
pre-treatment controls	✓	✓	✓	✓	✓
Observations	90,439	90,439	90,311	86,988	86,914
Adjusted R ²	0.815	0.816	0.815	0.819	0.820
	(6)	(7)	(8)	(9)	(10)
10 hot days	-0.122 (0.153)	-0.103 (0.194)	-0.675 (0.178)	-0.839 (0.262)	-1.100 (0.447)
10 cold days	-0.240 (0.226)	-0.558 (0.145)	-0.896 (0.388)	-1.640 (0.946)	-2.130 (0.806)
drop all controls	✓	✓	✓	✓	✓
Observations	93,452	93,452	93,452	93,452	93,452
Adjusted R ²	0.808	0.808	0.808	0.808	0.808

Notes: Unit of analysis: outcome years (2001, 2010, 2019) \times counties \times industries. All models inherit the county, state-year, industry-year fixed effects at specification (5) from Table 1. The regressions are weighted by the denominator of labor share, i.e., GDP minus proprietors' income. Standard errors in parentheses are clustered at the state level.

Measurements of labor shares. Table A-4 presents robustness checks using alternative proxies of labor share. Column (1) repeats the baseline specification. Column (2) uses the simple ratio of labor income to GDP, without excluding proprietors' income in the denominator, representing an extreme assumption that all proprietors' income is attributed to capital income. Column

(3) adopts the ratio of wage compensation plus proprietors' income to GDP, representing the opposite extreme assumption that all proprietors' income is attributed to labor income. The results are similar, suggesting that the treatment of proprietors' income has little influence on the findings.

Table A-4: By Measurements of Labor Shares

	dependent variables: labor shares (units: percentage points)		
	Baseline	No adjustment of proprietors' income	Proprietors' income added to labor income
	(1)	(2)	(3)
10 hot days	−0.589 (0.202)	−0.633 (0.173)	−0.466 (0.201)
10 cold days	−0.874 (0.414)	−0.958 (0.491)	−0.747 (0.378)
Observations	90,311	97,023	90,383
Adjusted R ²	0.815	0.736	0.810

Notes: Unit of analysis: outcome years (2001, 2010, 2019) \times counties \times industries. All models inherit the full controls and county, state-year, industry-year fixed effects at specification (5) from Table 1. The regressions are weighted by the denominator of labor share, i.e., GDP minus proprietors' income. Standard errors in parentheses are clustered at the state level.

Leave-one-out analysis. To address the concern that the results may be disproportionately influenced by specific industries or regions, we conduct a series of robustness checks by dropping the most temperature-sensitive or automatable industries or regions one at a time. Column (1) of Table A-5 reproduces the baseline estimates for reference and comparison. Columns (2)–(4) rerun the analysis, each time excluding one of the most outdoor-intensive industries: construction-mining-utilities, manufacturing, and transportation. The results confirm that no single industry disproportionately drives the observed effects.

Additionally, we assess the influence of specific regions. The NOAA climate regions, ranked by the number of hot days in 2019, are as follows: Southeast, South, Southwest, West, Central, Northeast, East North Central, West North Central, and Northwest. In Columns (5) and (6), we exclude the two hottest regions and two coldest regions, respectively. The results are barely changed, confirming that the findings are not driven by any particular region.

Table A-5: Dropping industries and regions

	dependent variable: labor share (units: percentage points)					
	Baseline	Drop construction, mining, utilities	Drop manufacturing	Drop transportation	Drop Southeast & South	Drop Northwest & West North Central
	(1)	(2)	(3)	(4)	(5)	(6)
10 hot days	−0.589 (0.202)	−0.484 (0.234)	−0.772 (0.116)	−0.535 (0.218)	−0.611 (0.195)	−0.664 (0.162)
10 cold days	−0.874 (0.414)	−0.878 (0.468)	−0.961 (0.527)	−0.786 (0.380)	−0.782 (0.388)	−1.000 (0.383)
Observations	90,311	79,196	82,259	84,601	56,891	79,848
Adjusted R ²	0.815	0.832	0.853	0.827	0.828	0.817

Notes: Unit of analysis: outcome years (2001, 2010, 2019) \times counties \times industries. All models inherit the full controls and county, state-year, industry-year fixed effects at specification (5) from Table 1. The regressions are weighted by the denominator of labor share, i.e., GDP minus proprietors' income. Standard errors in parentheses are clustered at the state level.

Fixed effects. In the baseline specification presented in Table 1, we include county fixed effects, state-year fixed effects, we include industry-year fixed effects. To ensure that our stringent inclusion of these fixed effects does not over-saturate the model, Table A-6 explores alternative ways to control for the dynamic trends of temperature warming and declining labor shares. Column (1) reproduces the baseline estimates for reference. Column (2) replaces industry-year fixed effects with only industry fixed effects. Column (3) controls for industry-specific time trends as an alternative to industry-year fixed effects. Column (4) controls for both industry fixed effects and division-specific time trends. Finally, Column (5) controls for both industry fixed effects and industry-specific time trends. The estimates remain consistent across specifications, regardless of the method used to account for the industry-specific time dynamics.

Nonlinear effects of extreme temperature. Table A-7 presents the nonlinear effects of more extreme temperatures using narrower bins relative to a normal range of 50°F to 77°F. The results indicate that hot days between 77°F and 90°F, as well as cold days between 40°F and 50°F, have significantly adverse effects on labor share. For the most extreme hot or cold days, however, the effects are less precisely estimated, likely due to a lack of statistical power stemming from the relatively low frequency of such weather events.

Table A-6: By Inclusion of Fixed Effects

	dependent variable: labor share (units: percentage points)				
	(1)	(2)	(3)	(4)	(5)
Baseline					
10 hot days	−0.589 (0.202)	−0.541 (0.162)	−0.607 (0.185)	−0.514 (0.150)	−0.554 (0.186)
10 cold days	−0.874 (0.414)	−0.875 (0.446)	−1.180 (0.501)	−0.889 (0.444)	−0.903 (0.422)
county FE	✓	✓	✓	✓	✓
state-year FE	✓	✓	✓	✓	✓
NAICS-year FE	✓	-	-	-	-
NAICS FE	-	✓	-	✓	✓
NAICS trend	-	-	✓	-	✓
division trend	-	-	-	✓	-
Observations	90,311	90,311	90,311	90,311	90,311
Adjusted R ²	0.815	0.804	0.711	0.806	0.810

Notes: Unit of analysis: outcome years (2001, 2010, 2019) \times counties \times industries. All models inherit the full controls at specification (5) from Table 1. Division consists of 6 broad industry groups mining, construction-utilities, manufacturing, retail, transportation and service. The regressions are weighted by the denominator of labor share, i.e., GDP minus proprietors' income. Standard errors in parentheses are clustered at the state level.

Table A-7: The Impacts of Severer Temperature

	dependent variable: labor share (units: percentage points)							
	(1)	(2)	(3)	(4)	(5)	(6)	(7)	(8)
hot days $\geq 77^\circ\text{F}$	-0.589 (0.202)					-0.572 (0.211)	-0.571 (0.217)	-0.555 (0.219)
[77, 80) $^\circ\text{F}$		-1.640 (0.611)	-1.480 (0.665)					
hot days $\geq 80^\circ\text{F}$		-0.322 (0.219)						
[80, 85) $^\circ\text{F}$			-0.654 (0.450)					
[77, 85) $^\circ\text{F}$				-0.979 (0.290)				
hot days $\geq 85^\circ\text{F}$			-0.163 (0.164)	-0.157 (0.169)				
[77, 90) $^\circ\text{F}$					-0.559 (0.273)			
hot days $\geq 90^\circ\text{F}$					-0.705 (0.674)			
cold days $< 50^\circ\text{F}$	-0.874 (0.414)	-0.791 (0.392)	-0.778 (0.374)	-0.801 (0.372)	-0.878 (0.423)			
[45, 50) $^\circ\text{F}$						-1.970 (0.853)	-1.970 (0.814)	
cold days $< 45^\circ\text{F}$						-0.537 (0.338)		
[40, 45) $^\circ\text{F}$							-1.110 (0.552)	
cold days $< 40^\circ\text{F}$							-0.398 (0.352)	
[40, 50) $^\circ\text{F}$								-1.650 (0.638)
[30, 40) $^\circ\text{F}$								-0.533 (0.492)
cold days $< 30^\circ\text{F}$								-0.175 (0.667)
Observations	90,311	90,311	90,311	90,311	90,311	90,311	90,311	90,311
Adjusted R ²	0.815	0.815	0.815	0.815	0.815	0.815	0.815	0.815

Notes: Unit of analysis: outcome years (2001, 2010, 2019) \times counties \times industries. All models inherit the full controls and county, state-year, industry-year fixed effects at specification (5) from Table 1. The regressions are weighted by the denominator of labor share, i.e., GDP minus proprietors' income. Standard errors in parentheses are clustered at the state level.

II.2 Heterogeneity

Sectoral-specific estimates. We extend the baseline model to allow for the estimated impacts of hot and cold days to vary across broad sectors: construction-mining-utilities, manufacturing, low-skilled services, and high-skilled services. This model with sectoral heterogeneity is specified as follows:

$$\text{LaborShare}_{l,k,\bar{I}} = \sum_K \mathbb{I}(K) (\beta_K^h \text{hd}_{l,I} + \beta_K^c \text{cd}_{l,I}) + \Lambda \mathbf{C}_{l,I} + \Gamma \mathbf{Z}_{l,k,\underline{I}} + \delta_l + \delta_{s,I} + \delta_{k,I} + \varepsilon_{l,k,\bar{I}}, \quad (\text{A1})$$

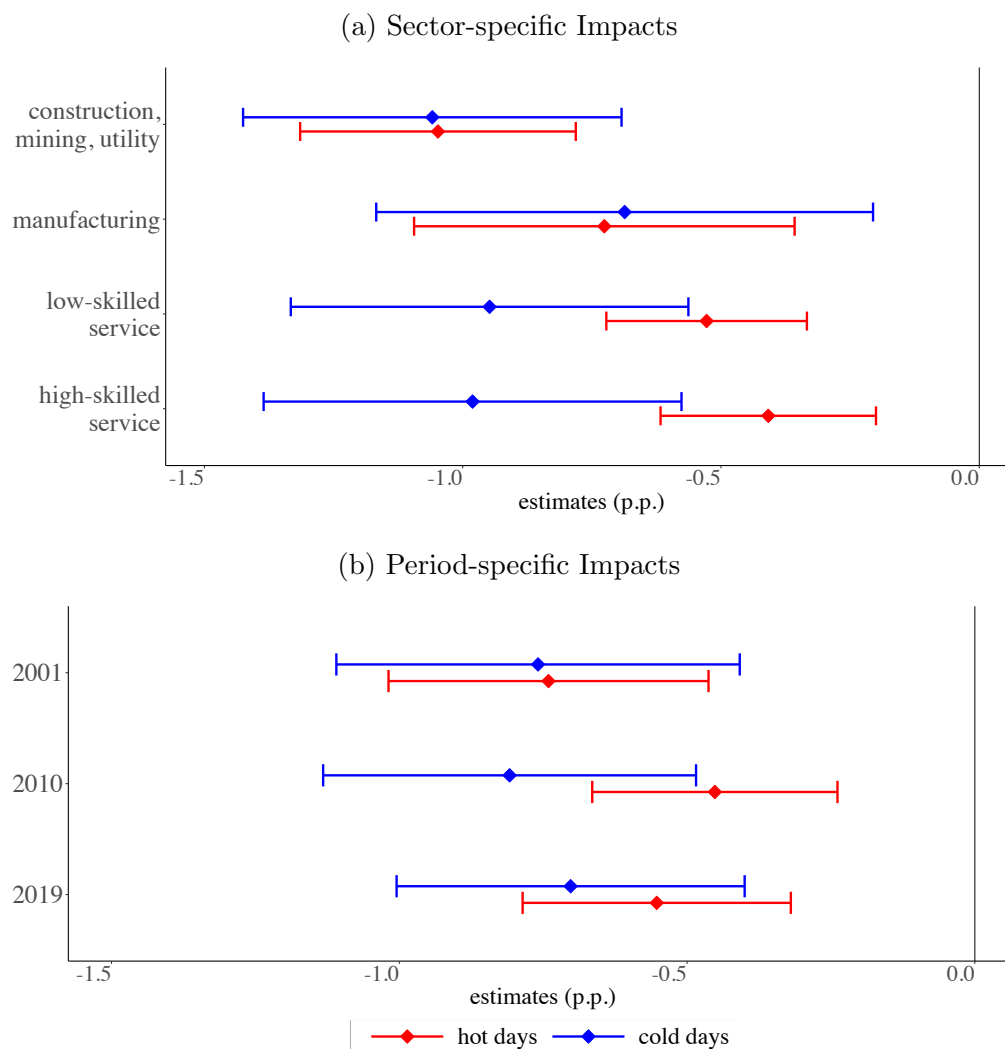
where the coefficients of the interaction terms with sector K dummies, β_K^h and β_K^c , capture the sector-specific impacts of hot and cold days, respectively. Figure A-8 presents these estimates in Panel (a).

Period-specific estimates. Alternatively, we extend the baseline model to allow for the estimated impacts of hot and cold days to vary across three periods, 1990–2001, 2001–2010, 2010–2019. The model with dynamically-variant effects is specified as follows

$$\text{LaborShare}_{l,k,\bar{I}} = \sum_I \mathbb{I}(I) (\beta_I^h \text{hd}_{l,I} + \beta_I^c \text{cd}_{l,I}) + \Lambda \mathbf{C}_{l,I} + \Gamma \mathbf{Z}_{l,k,\underline{I}} + \delta_l + \delta_{s,I} + \delta_{k,I} + \varepsilon_{l,k,\bar{I}}, \quad (\text{A2})$$

where the coefficients of the interaction terms with period I dummies, β_I^h and β_I^c , capture the period-specific estimates for hot and cold days, respectively. Figure A-8 presents these estimates in Panel (b).

Figure A-8: Models with Sector heterogeneity and Adaptation



Notes: Unit of analysis: outcome years (2001, 2010, 2019) \times counties \times industries. Both models inherit the full controls and county, state-year, industry-year fixed effects at specification (5) from Table 1. The regressions are weighted by the denominator of labor share, i.e., GDP minus proprietors' income. The horizontal bars represent the 95% confidence intervals using standard errors clustered at the state level.

II.3 Climate-Induced Automation

This section presents robustness checks and placebo checks to validate in the analyses conducted in Section 4.2.

Industry-level covariates. We construct industry k level covariates, consisting of other climate variables $\mathbf{C}_{k,I}$, industrial structure $\mathbf{S}_{k,I}$, demographic compositions $\mathbf{D}_{k,I}$, and other employment characteristics $\mathbf{M}_{k,I}$, for both analyses using BEA and IFR data.

- $\mathbf{C}_{k,I}$ includes average of daily precipitation on rainy days (intensive margin), the number of non-rainy days (extensive margin), and the number of days with heavy snowfall (≥ 300 mm) and relative humidity. (Source: GHCN-daily)
- $\mathbf{S}_{k,I}$ includes Herfindahl-Hirschman Index (HHI) and employment share of large establishments with over 1,000 employees. (Source: County Business Pattern)
- $\mathbf{D}_{k,I}$ includes employment compositions by education attainment: less than high school degrees, high school graduates, college graduates and above; a share of junior (aged 16–35), senior (aged 55 and above); a share of non-hispanic whites, immigrants (foreign-born, non-citizens), and gender. (Source: Census and American Community Survey)
- $\mathbf{M}_{k,I}$ includes per capita non-labor income, and the share of renting a house. (Source: Census and American Community Survey)

Temperature thresholds. For the analyses on robot stocks and investments, we conduct robustness checks with alternative temperature cutoffs defining hot and cold days. Table A-8 presents the robust checks for the BEA data and Table A-9 for the IFR data. Reassuringly, the results are robust to alternative cutoff choices.

Lagged climate effect on robot investments. The analysis in Panel A of Table 2 estimates the decadal impact of hot and cold days on end-of-treatment investments. Alternatively, Table A-10 examines how climate change affects future robot investment behaviors. To do so, we create a 5-year lag for the end year of the treatment period and outcome years \bar{I} in Columns (2)–(3) and (5)–(6). Specifically, Columns (2) and (5) take the 10-year average of hot and cold days, and Columns (3) and (6) take the 5-year average. For example, for the outcome year 2010, Columns (2) and (5) consider the average treatment over 1996–2005, and Columns (3) and (6) consider the average treatment over 2001–2005. Overall, the estimates are smaller than the baseline results in Columns (1) and (4), but retain statistical significance.

Table A-8: By Temperature Thresholds (industrial robots from the BEA)

	dependent variable: Robot/Capital (Units: percentage points)							
	(1)	(2)	(3)	(4)	(5)	(6)	(7)	(8)
hot days $\geq 70^{\circ}\text{F}$	3.690 (0.352)							
$\geq 75^{\circ}\text{F}$		3.070 (0.425)						
$\geq 77^{\circ}\text{F}$			2.740 (0.464)		2.450 (0.986)	2.980 (0.346)	2.780 (0.311)	2.100 (0.399)
$\geq 80^{\circ}\text{F}$				2.830 (0.781)				
cold days $< 50^{\circ}\text{F}$	5.200 (1.110)	4.230 (1.260)	3.810 (1.330)	3.650 (1.560)				
$< 55^{\circ}\text{F}$					2.660 (2.300)			
$< 45^{\circ}\text{F}$						5.270 (0.971)		
$< 40^{\circ}\text{F}$							6.480 (0.803)	
$< 35^{\circ}\text{F}$								6.850 (0.639)
Observations	200	200	200	200	200	200	200	200
Adjusted R ²	0.966	0.965	0.965	0.965	0.964	0.966	0.966	0.966

Notes: Unit of analysis: outcome years (1980–2010 by decades) \times industries. All models inherit the controls, division trend, and two-way fixed effects in specifications from Panel A of Table 3. The regressions are weighted by the industry-level GDP. Standard errors in parentheses are clustered at the division level.

Climate effect on capital. Table A-11 replicates the analysis using other capital measures that include equipment, structures, and IPP capitals. These results do not yield significant estimates.

Climate effect on digitization. Table A-12 replaces BEA robots with ICT capital and software and similarly does not produce significant estimates. In the National Income and Product Accounts (NIPA) from the BEA, ICT capital consists of PCs and mainframes, and software consists of prepackaged software, custom software, and own account software.

Table A-9: By Temperature Thresholds (industrial robots from the IFR)

	dependent variable: Robot / Capital (Units: robot stocks per 100 million USD)							
	(1)	(2)	(3)	(4)	(5)	(6)	(7)	(8)
hot days $\geq 70^\circ\text{F}$	9.010 (0.722)							
$\geq 75^\circ\text{F}$		10.000 (0.333)						
$\geq 77^\circ\text{F}$			8.810 (0.450)		6.180 (1.040)	7.780 (0.520)	6.570 (0.839)	5.070 (1.180)
$\geq 80^\circ\text{F}$				6.720 (0.582)				
cold days $< 50^\circ\text{F}$	11.000 (1.320)	11.900 (0.789)	10.400 (0.799)	7.640 (0.843)				
$< 55^\circ\text{F}$					6.860 (1.390)			
$< 45^\circ\text{F}$						9.970 (1.060)		
$< 40^\circ\text{F}$							8.730 (1.620)	
$< 35^\circ\text{F}$								7.400 (2.170)
Observations	51	51	51	51	51	51	51	51
Adjusted R ²	0.990	0.990	0.989	0.988	0.987	0.989	0.988	0.987

Notes: Unit of analysis: outcome years (2005, 2010, 2015) \times industries. All models inherit the controls, division trend, and two-way fixed effects in specifications from Panel B of Table 3. The regressions are weighted by the industry-level GDP. Standard errors in parentheses are clustered at the division level.

Table A-10: Lagged Climate Effects on Robot Investments (industrial robots from the BEA)

	Robot Inv./Capital Inv.			Robot Inv./GDP		
	(units: percentage points)					
	Baseline			Baseline		
	(1)	(2)	(3)	(4)	(5)	(6)
10 hot days (10 year)	4.830 (1.860)			1.170 (0.515)		
10 cold days (10 year)	7.560 (3.150)			1.450 (0.737)		
10 hot days (10 year, lag5)		2.210 (0.980)			0.434 (0.214)	
10 cold days (10 year, lag5)		3.230 (1.640)			0.373 (0.260)	
10 hot days (5 year, lag5)			3.180 (1.170)			0.791 (0.345)
10 cold days (5 year, lag5)			6.250 (2.380)			1.150 (0.542)
Observations	200	200	200	200	200	200
Adjusted R ²	0.939	0.935	0.939	0.846	0.838	0.845

Notes: Unit of analysis: outcome years (1980–2010 by decades) \times industries. All models inherit the controls, division trend and two-way fixed effects in specifications from Panel A of Table 3. The regressions are weighted by the industry-level GDP. Standard errors in parentheses are clustered at the division level.

Table A-11: Climate Impact on Capital Deployment by Broad Categories

	Equip. /Capital	Structure /Capital	IPP /Capital	Equip. Inv. /Capital Inv.	Structure Inv. /Capital Inv.	IPP Inv. /Capital Inv.
	(Units: percentage points)					
	(1)	(2)	(3)	(4)	(5)	(6)
10 hot days	1.700 (3.740)	−3.360 (4.250)	1.670 (1.900)	4.420 (5.580)	−8.510 (3.630)	4.090 (5.210)
10 cold days	0.308 (1.810)	4.270 (1.510)	−4.580 (1.320)	6.760 (3.210)	−5.320 (3.580)	−1.440 (1.270)
Observations	200	200	200	200	200	200
Adjusted R ²	0.949	0.971	0.960	0.911	0.923	0.947

Notes: Unit of analysis: outcome years (1980-2010 by decades) \times industries. All models inherit the controls, division trend and two-way fixed effects in specifications from Panel A of Table 3. The regressions are weighted by the industry-level GDP. Standard errors in parentheses are clustered at the division level.

Table A-12: Climate Impact on Digitization

	ICT /Capital	Software /Capital	ICT Inv. /Capital Inv.	Software Inv. /Capital Inv.
	(Units: percentage points)			
	(1)	(2)	(3)	(4)
10 hot days	−0.129 (0.130)	−0.729 (2.440)	−0.509 (0.393)	0.234 (6.490)
10 cold days	0.167 (0.162)	−4.300 (1.210)	0.476 (0.544)	−3.850 (1.510)
Observations	200	200	200	200
Adjusted R ²	0.915	0.836	0.841	0.888

Notes: Unit of analysis: outcome years (1980-2010 by decades) \times industries. All models inherit the controls, division trend and two-way fixed effects in specifications from Panel A of Table 3. The regressions are weighted by the industry-level GDP. Standard errors in parentheses are clustered at the division level.

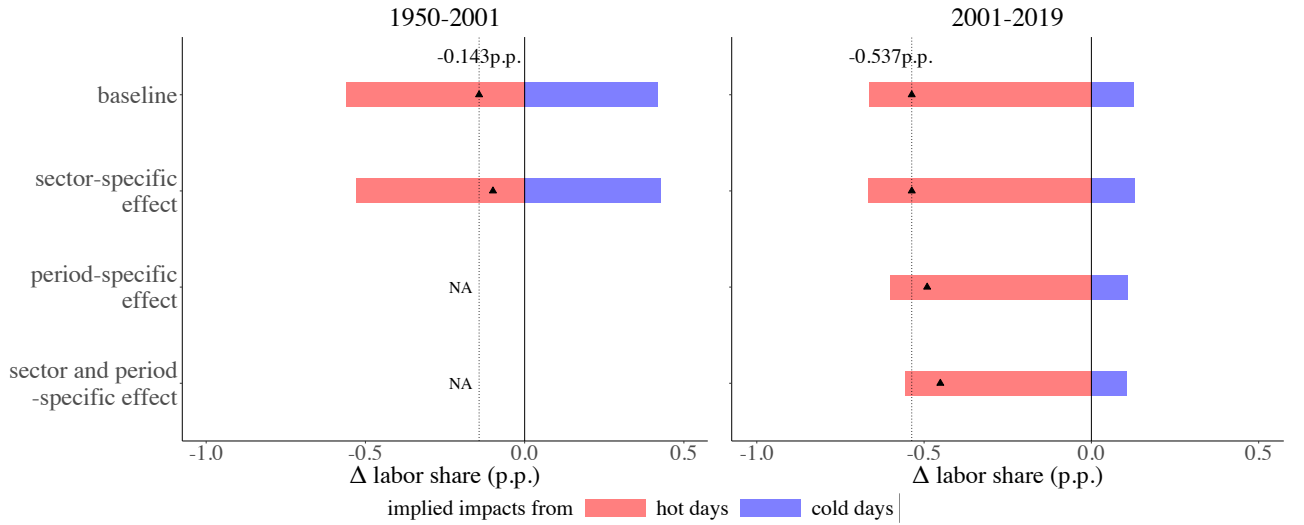
II.4 Assessment of Macroeconomic Impacts

Robustness checks of assessment. Figure A-9 presents robustness checks using alternative models to assess the macroeconomic impacts. Specifically, these models incorporate heterogeneity by periods and sectors to provide a more nuanced analysis. The first row of Figure A-9 replicates the assessment using the baseline estimates, β^h and β^c . The second row applies sector-specific estimates, β_K^h and β_K^c from Panel (a) of Figure A-8. The third row applies period-specific estimates, β_I^h and β_I^c from Panel (b) of Figure A-8. Finally, the fourth row uses a hybrid model that allows for sector-by-period specific estimates $\beta_{K,I}^h$ and $\beta_{K,I}^c$ from the following augmented regression:

$$\text{LaborShare}_{l,k,\bar{I}} = \sum_I \sum_K \mathbb{I}(I)\mathbb{I}(K) (\beta_{K,I}^h \text{hd}_{l,I} + \beta_{K,I}^c \text{cd}_{l,I}) + \mathbf{\Lambda} \mathbf{C}_{l,I} + \mathbf{\Gamma} \mathbf{Z}_{l,k,\underline{I}} + \delta_l + \delta_{s,I} + \delta_{k,I} + \varepsilon_{l,k,\bar{I}}. \quad (\text{A3})$$

Reassuringly, the macroeconomic implications derived from these alternative models remain consistent with the baseline results.

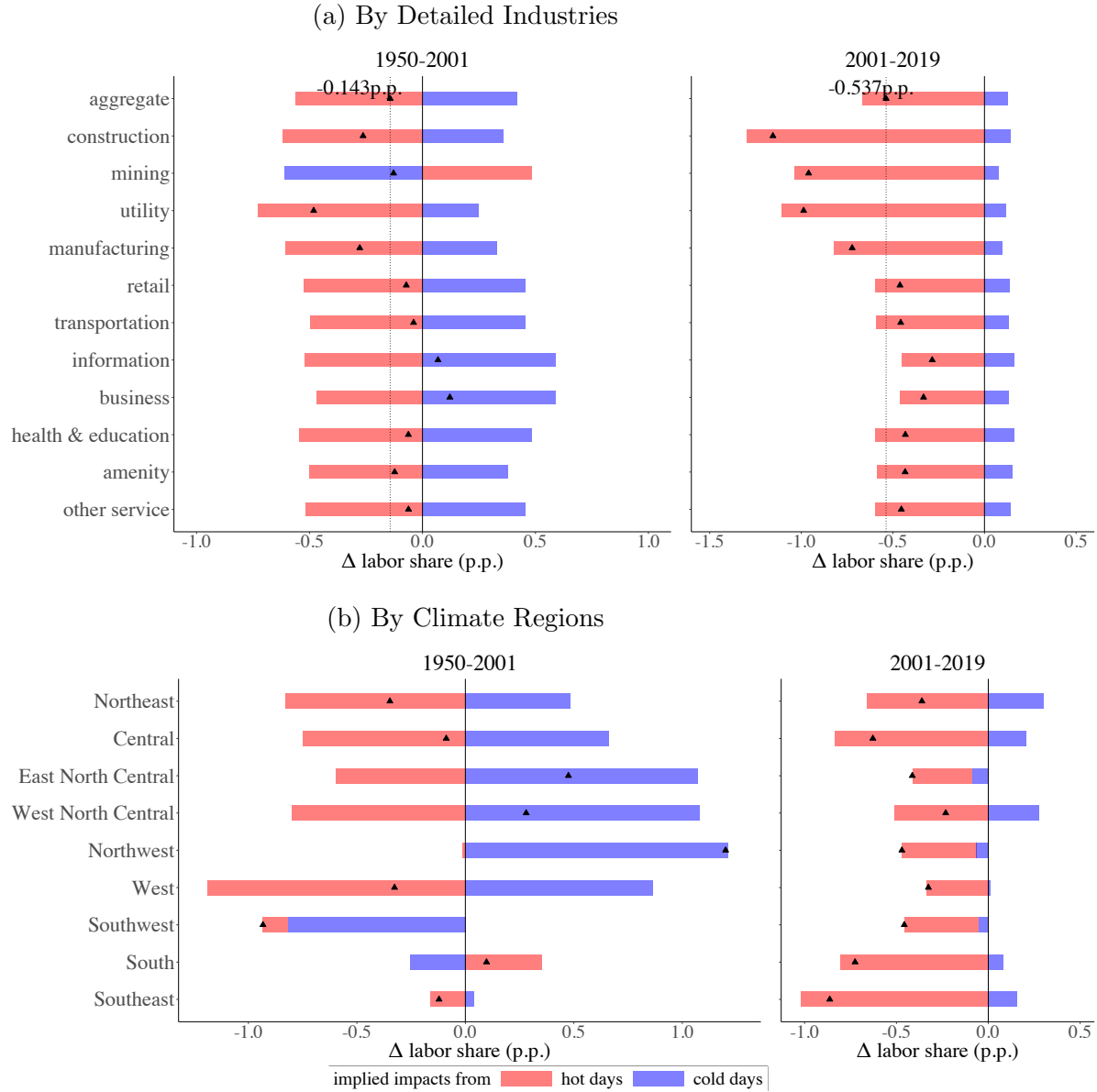
Figure A-9: Robustness Checks of Assessment across Modeling Choices



Notes: Black triangles mark the net effects of hot and cold days. The baseline results are calculated using the estimates from Column (5) in Table 1. Sector-specific and period-specific effects are derived from Panels (a) and (b) of Figure A-8, respectively. The sector-and-period-specific effects are based on the estimates from Equation (A3). In the third and fourth rows, the assessment is unavailable due to the absence of corresponding period-specific estimates for the years 1950–2001.

Implied impacts by industries and climate regions. Figure A-10 presents the implied impacts of climate change across 11 industries and 9 NOAA climate regions. These impacts are calculated using the sector-specific estimates from Panel (a) of Figure A-8, providing a detailed breakdown of climate effects by industry and region.

Figure A-10: Implied Impacts of Climate Change on Labor Shares



Notes: Black triangles mark the net effects of hot and cold days. The implied impacts are calculated using the four broad sector-specific estimates from Equation (A1). Panel (a): Dotted vertical lines represent the nationwide net climate impacts. Industries correspond to BEA-based NAICS classifications. Panel (b): Climate regions are defined according to NOAA classifications.